Journal of Frontiers in Multidisciplinary Research

Modeling Cell Dynamics and Epigenetic Transitions. From Agent-Based to transport frameworks

Manuel Doblaré [1*], Marina Pérez-Aliacar [2], Jacobo Ayensa-Jiménez [3]
[1,2,3] TME Lab, Aragón Institute of Engineering Research (I3A), University of Zaragoza, Zaragoza, Spain
[1, 2] Aragón Institute for Health Research (IIS Aragón), Zaragoza, Spain
[1] CIBER-BBN, ISCIII
[1] Sino-Spain Joint Laboratory on Biomedical Materials (S2BLM), College of Materials Science and Engineering, Nanjing Tech University, Nanjing, China
[3] Polytechnic University of Madrid, Madrid, Spain

* Corresponding Author: **Manuel Doblaré**

Article Info

E-ISSN: 3050-9726
P-ISSN: 3050-9718
Volume: 07
Issue: 02
Received: 10-07-2026
Accepted: 08-08-2026
Published: 06-09-2026
Page No: 242-258

Abstract
Epigenetic regulation is a fundamental component of biological organization, governing how genetically identical cells develop and maintain distinct behavior in response to the same external stimuli. Understanding how these mechanisms evolve has therefore become a central question in developmental biology, immunology, and oncology. Starting from a biological overview of epigenetics and its significance, we explore how different modeling paradigms—from discrete to continuum—represent cell and epigenetic evolution.
When a continuum epigenetic spectrum is considered, two main strategies are used. In the first, the physical space is expanded with additional epigenetic dimensions that describe the phenotypic space. Cells evolve in time through reaction-diffusion equations, occupying subsequent positions within that extended space, like standard Eulerian formulations in Continuum Physics. The second defines the epigenetic state by a set of internal variables carried by each cell representative volume that now evolves along time trajectories. This strategy may be interpreted as discretizing the epigenetic state continuous representation into a few discrete variables whose evolution is tracked along time.
In this work, we present these two approaches and formulate them under both Eulerian and Lagrangian viewpoints, focusing first on cellular evolution and subsequently extending the framework to include adaptation and phenotypic plasticity. Building upon this general framework, we review and discuss various procedures found in the literature for modeling epigenetic changes in cell populations. This comparative analysis establishes a coherent foundation for hybrid (discrete-continuous phenotypes) and multiscale models, while elucidating the fundamental differences between existing modeling frameworks.

DOI: https://doi.org/10.54660/.JFMR.2026.7.2.242-258

Keywords: Epigenetic changes modeling, Internal variables, Structural models, Lagrangian versus Eulerian formulations, Transport Phenomena

1. Introduction

Cells are complex dynamic systems in which genetic information, environmental cues, and stochastic fluctuations interact in a nonlinear manner, controlling processes like proliferation, migration, apoptotic or necrotic death, cell differentiation, or tissue production/resorption [1]. Epigenetics refers to the varied set of molecular mechanisms that regulate gene transcription without altering the underlying DNA sequence [2]. This regulation occurs through processes like DNA methylation, histone acetylation and methylation, nucleosome remodeling, chromatin compaction, and large-scale reorganization of three-dimensional genome architecture [3, 4]. Together with DNA programming, they shape cellular identity (phenotype) and specific cell history (epigenetic markers accumulation), determining how a particular cell responds to external stimuli and stores information about past

exposures [5,6]. These mechanisms endow cells with a form of molecular memory, which is partially reversible and heritable [2] thus, contributing to cellular plasticity, a property central to many biological processes like embryonic development [7], immune adaptation [8] or cancer progression [9].

Predicting how these modifications evolve in time and space is therefore essential to understand how cells maintain healthy tissue homeostasis as well as the progression and treatment of disease [10]. Given the complexity of these processes, with multiple spatial and temporal scales involved, computational modeling has become key to interpret and predict single cell and cell population evolution under varying environmental stimuli or therapeutic interventions. Computational models allow virtual experimentation, connecting microscopic biochemical events to macroscopic observables such as tissue growth, shape conformation, or cellular heterogeneity. In particular, when referring to epigenetic evolution, mathematical models help to elucidate how local enzymatic reactions and feedback loops in chromatin can lead to global patterns of cell-state transitions [11, 12], or how environmental factors such as hypoxia and drug exposure reshape the epigenetic landscape of tumors, including cell heterogeneity and resistance acquisition [13, 14, 15, 16].

Computational representations of cellular evolution typically follow two paradigms: discrete and continuous. Discrete models represent individual cells as autonomous entities whose behavior is governed by probabilistic or rule-based dynamics [17, 18]. They naturally capture stochasticity, heterogeneity, and local interactions, and incorporate explicitly intracellular mechanisms such as gene regulatory networks or epigenetic circuits. However, they are computationally expensive for large populations and often difficult to analyze mathematically. In contrast, continuous models describe the behavior of a whole cell population in terms of averaged fields, such as density, mean velocity, or mean internal state, that evolve in space and time under conservation laws and phenomenological constitutive relations [19, 20]. While these formulations lack internal molecular details, they are well suited for large-scale simulations, allow for systematic mathematical analysis and link directly to continuum theories of tissue biophysics thus, permitting to model macroscopic systems.

A similar duality arises when modeling the cell state evolution. Some formulations consider discrete transitions between a limited set of phenotypic states through stochastic or deterministic rules [21, 22]. While intuitive and easily tractable, such representations cannot reproduce the real gradual accumulation and erasure of epigenetic information [23, 24]. More realistic models introduce continuous epigenetic variables reflecting the smooth progressive transition of transcriptional shifts. This continuity gives rise to a landscape of cell states that are not discrete but arranged along a continuous manifold in which cells occupy intermediate, metastable positions.

Within this continuous paradigm, two major strategies have been proposed. The first attaches to each cell or cell cluster in a representative volume (cell RVE) a set of internal variables that describe the epigenetic state and whose evolution depends upon the local environmental cues and kinetic laws, as well as the epigenetic state itself [13, 14]. The second considers the epigenetic variables as continuous distributions. In these models, each epigenetic variable is assimilated to a new independent coordinate, additional to the spatial ones thus, extending the physical space that now includes the epigenetic continuous manifold. The cell population evolves in this augmented spatio-epigenetic domain through transport and reaction equations [25, 15].

Although conceptually distinct, these two formulations describe the same phenomenon from different perspectives. In the independent-variable picture, the focus lies on the evolution of the population density and fluxes observed at fixed points in the extended space, highlighting the spatio-temporal evolution of the epigenetic state field. In the dependent-variable picture, one follows individual trajectories of material points (cell RVE), carrying their internal variables as they evolve. Recognizing this equivalence allows for a unified interpretation of models that have been often considered as different in biological contexts.

The main objectives of this work are therefore to review the main formulations of cell dynamics models from both continuum and discrete perspectives and to examine how phenotypic evolution is incorporated into these frameworks. Furthermore, we evaluate its conceptual and computational characteristics, establish the relations between the variables used in each approach, and identify the biological scenarios where each of them is more appropriate.

The paper is organized as follows. Section 2 discusses the discrete and continuous computational perspectives for modeling cellular processes without considering epigenetics. This is useful to introduce concepts and formulations that are extended in section 3 to discrete and continuous representations of epigenetic and phenotype dynamics. We also review different families of epigenetic models that can be found in literature. Under this light, we discuss in section 4 their respective advantages, disadvantages and limitations for each specific application. In this same section, we summarize the relations between the different variables that appear in discrete and continuous models and between Eulerian and Lagrangian approaches for the latter. Finally, Section 5 discusses the main conclusions and conceptual contributions of this work, and some perspectives for future research.

2. Modeling Cellular Processes without Cell State Changes

Cells are living systems whose behavior emerges from the interplay of molecular reactions, gene regulation, biophysical signaling pathways, and physical interactions with neighboring cells and the extracellular matrix. Processes like proliferation and death, differentiation, migration, shape change, or new tissue production/resorption are fundamental events that drive tissue homeostasis, growth, morphogenesis, and disease. Understanding and predicting how these processes evolve is therefore key for biological processes like regenerative medicine, cancer therapy, developmental biology, or tissue engineering [26, 27, 28, 29].

Two broad paradigms dominate physically-based computational models of cell population behavior: discrete (agent-based) and continuous (field-based) approaches. Each embodies a different balance between mechanistic detail, computational cost, and analytical tractability. Finally, machine learning (ML) approaches complement the above by learning predictive mappings between inputs and outputs directly from data [30, 31] or combining physics and data in hybrid frameworks such as Physics-Informed Neural Networks (PINNs) [32, 33]. Although the integration of purely data-driven models with classical biologically-based approaches promises to accelerate discovery and enhance predictive power in systems biology, in the following we shall focus only on the latter.

2.1. Modeling Cell Populations with a Numerable Number of Cells

Discrete models represent cells as individual entities that carry properties like position, velocity, or phenotypic state that evolve over time according to specific rules, with the aim of defining the value of each of those properties at each time instant. They also account for cell appearance and disappearance due to division or death, as well as entry into or exit from the domain.

Discrete cell-based models encompass a broad class of approaches, including cellular automata, lattice-based models, and off-lattice individual-based formulations. Among these, we focus on Agent-Based Models (ABMs) [34, 35] which describe the coupled behavior of a set of agents, here identified with cells, that make decisions autonomously according to prescribed rules based on both external signals and their internal state. ABMs are suitable for modeling tumor evolution incorporating heterogeneity [36, 37] as well as epigenetic regulation and adaptation, as we will see in the next section. In particular, ABMs naturally capture cell-to-cell heterogeneity, allow for the incorporation of internal variables representing epigenetic states and cell state, and provide a flexible framework to model history-dependent behavior and memory effects at the single-cell level.

Within this framework, each cell k is characterized by its position $\boldsymbol{x}^k(t) \in \Omega_{\boldsymbol{x}} \subset \mathbb{R}^3$ that evolves over the simulated time interval I. Cell dynamics arise from key biological processes such as proliferation, death, migration, and phenotypic or epigenetic transitions.

Cell proliferation and death are typically modeled through transition probabilities between discrete states (representing, for example, different phases in the cell cycle), often described as Markov processes. Cell migration may be modeled either on a lattice, considering only a discrete number of sites that can be occupied according to probabilistic rules [38], or in a continuous space (off-lattice models) [17, 39], where cell movement is governed by a velocity $\boldsymbol{v}^k$ that depends on both the internal state and environmental cues. A common representation combines directed and random components:

$$\boldsymbol{v}^k = A\boldsymbol{u} + B\boldsymbol{\zeta}, \qquad (1)$$

where $\boldsymbol{\zeta}$ is a unit vector with random direction, and $\boldsymbol{u}$ a unit vector indicating the direction of biased migration induced by the combined action of different taxes and drag forces, while A, B define the amplitude of these two components of the velocity, that may depend on the value of such taxes and the cell state. This equation must be solved simultaneously for all cells, having therefore a discrete number of Ordinary Differential Equations (ODEs), associated with the evolution of each cell k in space, which provides its location $\boldsymbol{x}^k(t) \in \mathbb{R}^3$ at time t.

Overall, cell evolution in ABMs (and discrete models in general) adopts a material description in which variables are associated to individual cells, enabling direct access to single-cell dynamics at every time t.

2.2. Modeling Cell Populations with a Continuous Cell Density

Continuous models take the complementary viewpoint by describing cell populations as continuous fields of averaged variables. These approaches, by their very nature, smooth out discrete events and individual fluctuations, so they are good to elucidate mechanisms of pattern formation, tissue growth, and invasion waves in tumor invasion [28, 20], but fail when cell number is small or cell response is mainly driven by stochastic effects. Indeed, macroscopic continuous fields can be obtained from ABM models using mean field thermodynamics.

Continuous models are typically expressed in terms of systems of partial differential equations derived from conservation laws. Two alternative but equivalent perspectives are used to describe the evolution of continuous systems: the Eulerian and Lagrangian formulations [40, 41]. Their conceptual distinction lies in the respective frame of reference: while the Eulerian framework describes the time evolution of field variables in a fixed space, the Lagrangian framework follows individual small volumes of material (points in the continuum formulation) as they move and change over time.

Eulerian Description

Using the general transport theorem, we can formulate the Eulerian differential version of the change rate for cell concentration, as

$$\frac{\mathrm{D}c(\boldsymbol{x},t)}{\mathrm{D}t} + c(\boldsymbol{x},t)\,\mathrm{div}_{\boldsymbol{x}}\,\boldsymbol{v}(\boldsymbol{x},t) + \mathrm{div}_{\boldsymbol{x}}\,\boldsymbol{q}_{\mathrm{d}}\,(\boldsymbol{x},t) =$$

$$c(\boldsymbol{x},t)\big[r_{\mathrm{p}}(\boldsymbol{x},t) - r_{\mathrm{d}}(\boldsymbol{x},t)\big], \qquad (2)$$

where $\frac{\mathrm{D}}{\mathrm{D}t}$ is the so-called material derivative or total derivative with respect to time, that omitting the dependencies for the sake of clarity is expressed as

$$\frac{\mathrm{D}c(\boldsymbol{x},t)}{\mathrm{D}t} = \frac{\partial c(\boldsymbol{x},t)}{\partial t} + \boldsymbol{v}\cdot\mathrm{grad}_{\boldsymbol{x}}c, \qquad (3)$$

and $\boldsymbol{v}(\boldsymbol{x},t)$ the spatial advection velocity of cells at point $\boldsymbol{x}$ and time t that depends on the external signals (taxes) and the state of the cells, becoming clear that we need to assume that all cells in a cell RVE ($\boldsymbol{x}$) have the same velocity. Also, r_{p} is

the rate of proliferation (rate of new cells production per unit cell) at $\boldsymbol{x}$ and t, and subjected to environmental signals \mu $\mu(\boldsymbol{x}, t)$ (whose evolution may also be described with a reaction-diffusion equation), while r_{d} is the rate of death by necrosis or apoptosis. These values can be modeled with different degree of detail, from just predefined functions fitted from available data to very complicated models encompassing the intrinsic cell or molecular mechanisms involved [42]. The term $\boldsymbol{q}_{\mathrm{d}}$ is the diffusive flux of cells, that is, cells entering the reference volume through its surface (cells per unit time and unit surface) due to diffusion or pedesis (random movement of cells) and is an emergent term appearing from thermodynamic averaging. Thus, the explicit dependencies of each variable that we will omit from now on for clarity purposes are the following:

$$\begin{aligned}
&\boldsymbol{q}_{\mathrm{d}}(\boldsymbol{x}, t) = \boldsymbol{q}_{\mathrm{d}}(\boldsymbol{x}, t, c(\boldsymbol{x}, t)),\\
&r_{\mathrm{p}}(\boldsymbol{x}, t) = r_{\mathrm{p}}(\boldsymbol{x}, t, c(\boldsymbol{x}, t), \boldsymbol{\mu}(\boldsymbol{x}, t)),\\
&r_{\mathrm{d}}(\boldsymbol{x}, t) = r_{\mathrm{d}}(\boldsymbol{x}, t, c(\boldsymbol{x}, t), \boldsymbol{\mu}(\boldsymbol{x}, t)).
\end{aligned}$$

We can express the advection flux as $\boldsymbol{q}_{\mathrm{a}}(\boldsymbol{x}, t) = c\boldsymbol{v}$, and using $\mathrm{div}_{\boldsymbol{x}}(c\boldsymbol{v}) = c\ \mathrm{div}_{\boldsymbol{x}}(\boldsymbol{v}) + \boldsymbol{v} \cdot \mathrm{grad}_{\boldsymbol{x}} c$, Equation (2) can be rewritten in the conservative form as:

$$\frac{\partial c}{\partial t} + \mathrm{div}_{\boldsymbol{x}}(\boldsymbol{q}_{\mathrm{a}} + \boldsymbol{q}_{\mathrm{d}}) = cr, \qquad (4)$$

where the source term is $r = r_{\mathrm{p}} - r_{\mathrm{d}}$.

If we assume a simple linear diffusion model, we have, in the end,

$$\frac{\partial c}{\partial t} + \mathrm{div}_{\boldsymbol{x}}\boldsymbol{q}_{\mathrm{a}} = cr + \mathrm{div}_{\boldsymbol{x}}(\boldsymbol{D}_c \mathrm{grad}_{\boldsymbol{x}} c), \qquad (5)$$

being $\boldsymbol{D}_c$ the diffusion tensor.

We therefore need to make explicit the diffusion matrix $\boldsymbol{D}_c$ at each point $\boldsymbol{x}$ as well as the reaction function, r, and the advection flux, $\boldsymbol{q}_{\mathrm{a}}$. This latter may be obtained after defining or computing two velocities. First, the advection velocity must be determined at each point (e.g. solving a fluid flow or solid deformation problem to get the distribution of drag forces or velocities acting on the cells at every spatial point and time due to the surrounding solid or fluid velocity). Second, a phenomenological expression is required for the intrinsic cell movement due to external signals (taxes). If we also want to model the evolution of the concentration of these signals, such as oxygen or other nutrients, this can be expressed in terms of transport equations for each species or signal μ_{i}, which in Eulerian form write:

$$\frac{\partial \mu_i}{\partial t} + \mathrm{div}_{\boldsymbol{x}}(\mu_i \boldsymbol{v}) = \mathrm{div}_{\boldsymbol{x}}(\boldsymbol{D}_i \mathrm{grad}_{\boldsymbol{x}} \mu_i) + s_i, \qquad (6)$$

where, here, a simple linear diffusion is considered. Finally, s_i is the source term for species i that comprises decay as well as production and/or consumption by cells, being expressed as:

$$s_i = -d_i \mu_i + \alpha_i c, \qquad (7)$$

with d_i the decay rate, and α_i the function modeling the net production/consumption rate of each species by cells located at point $\boldsymbol{x}$ at time t.

This context is well suited for describing flows, diffusion, and reactions making abstraction of the actual evolution of properties of the individual cells composing the system. It is, therefore, particularly useful for problems where the precise location of individual cells is less relevant than the spatio-temporal evolution of key concentrations. Such an approach is ideal for studying the emergence of biological patterns, as seen in morphogenesis [43], tumor growth [20], and the dynamics of heterogeneous cell populations [44, 45]. However, we cannot follow directly the history of the variables associated to each cell (velocity, position, state, ...) since the cells passing through a certain fixed point $\boldsymbol{x}$ change over time. This makes it more complex to account for history-dependent behaviors, particularly in processes driven by the evolution of the epigenetic state. While certain techniques can mitigate this problem by incorporating additional state variables, they significantly increase model complexity; therefore, a Lagrangian description is often more suitable for such cases.

Lagrangian Description

The Lagrangian approach focuses on following each material point, usually defined by its coordinates $\boldsymbol{X}$ at an initial time $t = t_0$, along its trajectory through space and time. Rather than examining what happens at fixed spatial coordinates, one tracks how properties attached to each cell RVE, such as position, velocity, cell concentration or internal state, change as it moves and evolves. In this case, the initial position of each point of the domain of interest must be explicitly defined, like in the discrete case.

To derive the governing equations in this framework, we first establish the motion mapping $\boldsymbol{x} = \boldsymbol{\chi}(\boldsymbol{X}, t)$, which links the reference configuration to the current position and is obtained from the definition of the velocity field for all material points $\boldsymbol{V}(\boldsymbol{X}, t) = \boldsymbol{v}(\boldsymbol{\chi}(\boldsymbol{X}, t), t)$. The deformation of the domain is characterized by the deformation gradient $\boldsymbol{F} = \frac{\partial \boldsymbol{x}}{\partial \boldsymbol{X}}$ and its determinant, the Jacobian $J = \det \boldsymbol{F}$, which represents the local volume change. The material cell concentration is then defined as $C(\boldsymbol{X}, t) = Jc(\boldsymbol{x}, t)$, representing the number of cells per unit of material reference volume. By applying the Reynolds Transport Theorem in its differential form, the Eulerian conservation law (Eq. 4) is pulled back to the reference configuration. In this description, the material derivative simplifies to the partial derivative with respect to time, $\frac{\mathrm{D}}{\mathrm{D}t} = \frac{\partial}{\partial t}$, and the advective terms are implicitly handled by the motion of the coordinate system. The key identity, which follows directly from the definition $C = Jc$ and the material time derivative of J:

$$\left.\frac{\partial C}{\partial t}\right|_{\boldsymbol{X}} = \left.\frac{\partial (Jc)}{\partial t}\right|_{\boldsymbol{X}} = J\left(\left.\frac{\partial c}{\partial t}\right|_{\boldsymbol{x}} + \mathrm{div}_{\boldsymbol{x}}(c\boldsymbol{v})\right),$$

allows us to identify the left-hand side of (4), with $\boldsymbol{q}_{\mathrm{a}}(\boldsymbol{x}, t) = c\boldsymbol{v}$, after separating the advective and diffusive fluxes, as:

$$\left.\frac{\partial c}{\partial t}\right|_{\boldsymbol{x}} + \mathrm{div}_{\boldsymbol{x}}\boldsymbol{q}_{\mathrm{a}} = \frac{1}{J}\left.\frac{\partial C}{\partial t}\right|_{\boldsymbol{X}}.$$

Multiplying (4) by J and applying the Piola identity $J\mathrm{div}_{\boldsymbol{x}}\boldsymbol{b} = \mathrm{DIV}_{\boldsymbol{X}}(J\boldsymbol{F}^{-1}\boldsymbol{b})$ to the diffusive flux:

$$J\mathrm{div}_{\boldsymbol{x}}\boldsymbol{q}_{\mathrm{d}} = \mathrm{DIV}_{\boldsymbol{X}}(J\boldsymbol{F}^{-1}\boldsymbol{q}_{\mathrm{d}}) = \mathrm{DIV}_{\boldsymbol{X}}\boldsymbol{Q}_{\mathrm{d}},$$

where the material diffusive flux is defined as $\boldsymbol{Q}_{\mathrm{d}} = J\boldsymbol{F}^{-1}\boldsymbol{q}_{\mathrm{d}}$. The advective terms are implicitly handled by the motion of the coordinate system, and the balance equation becomes:

$$\frac{\partial C(\boldsymbol{X},t)}{\partial t} + \mathrm{DIV}_{\boldsymbol{X}}\boldsymbol{Q}_{\mathrm{d}} = C(\boldsymbol{X},t)\left[R_{\mathrm{p}}(\boldsymbol{X},t) - R_{\mathrm{d}}(\boldsymbol{X},t)\right], \quad (8)$$

where the material counterparts of c,r_{p},r_{d} and $\boldsymbol{q}_{\mathrm{d}}$, defined per unit volume of the initial configuration are:

$$\begin{aligned}
&C(\boldsymbol{X},t) = Jc(\boldsymbol{\chi}(\boldsymbol{X},t),t),\\
&\boldsymbol{Q}_{\mathrm{d}}(\boldsymbol{X},t) = J(\boldsymbol{X},t)\boldsymbol{F}^{-1}(\boldsymbol{X},t)\boldsymbol{q}_{\mathrm{d}}(\boldsymbol{\chi}(\boldsymbol{X},t),t,C(X,t)),\\
&R_{\mathrm{p}}(\boldsymbol{X},t) = r_{\mathrm{p}}(\boldsymbol{\chi}(\boldsymbol{X},t),c(\boldsymbol{\chi}(\boldsymbol{X},t),t),\boldsymbol{\mu}(\boldsymbol{\chi}(\boldsymbol{X},t),t),t),\\
&R_{\mathrm{d}}(\boldsymbol{X},t) = r_{\mathrm{d}}(\boldsymbol{\chi}(\boldsymbol{X},t),c(\boldsymbol{\chi}(\boldsymbol{X},t),t),\boldsymbol{\mu}(\boldsymbol{\chi}(\boldsymbol{X},t),t),t),
\end{aligned}$$

The material flux $\boldsymbol{Q}_{\mathrm{d}}$ accounts for the transformation of the diffusive flux vector from the deformed spatial configuration back to the reference state. If we assume a simple linear diffusion model, using the transformation of the spatial gradient, $\mathrm{grad}_{\boldsymbol{x}}c = \boldsymbol{F}^{-\mathrm{T}}\mathrm{GRAD}_{\boldsymbol{X}}\left(\frac{C}{J}\right)$, and substituting into the definition of $\boldsymbol{Q}_{\mathrm{d}}$:

$$\begin{aligned}
&\boldsymbol{Q}_{\mathrm{d}} = J\boldsymbol{F}^{-1}\boldsymbol{q}_{\mathrm{d}} = -J\boldsymbol{F}^{-1}\boldsymbol{D}_c\mathrm{grad}_{\boldsymbol{x}}c\\
&= -J\boldsymbol{F}^{-1}\boldsymbol{D}_c\boldsymbol{F}^{-\mathrm{T}}\mathrm{GRAD}_{\boldsymbol{X}}\left(\frac{C}{J}\right)
\end{aligned}$$

which can be written compactly as:

$$\boldsymbol{Q}_{\mathrm{d}} = -J\boldsymbol{D}_C\mathrm{GRAD}_{\boldsymbol{X}}\left(\frac{C}{J}\right), \quad (9)$$

with

$$\boldsymbol{D}_C = \boldsymbol{F}^{-1}\boldsymbol{D}_c\boldsymbol{F}^{-\mathrm{T}} \quad (10)$$

the material diffusion tensor. Substituting into (8) yields the closed material balance equation:

$$\frac{\partial C}{\partial t} = CR + \mathrm{DIV}_{\boldsymbol{X}}\left[J\boldsymbol{D}_C\mathrm{GRAD}_{\boldsymbol{X}}\left(\frac{C}{J}\right)\right], \quad (11)$$

where $R = R_{\mathrm{p}} - R_{\mathrm{d}}$ is the net material reaction rate.

Analogously, we can derive the Lagrangian equation for the evolution of the chemical species. We define the material concentration of the i-th species as $M_i(\boldsymbol{X},t) = \mu_i(\boldsymbol{\chi}(\boldsymbol{X},t),t)$. Unlike the cell concentration $C = Jc$, the species concentration μ_i is an intensive quantity, so its material counterpart carries no Jacobian factor. Expanding the divergence in (6) using the product rule:

$$\frac{\partial \mu_i}{\partial t} + \boldsymbol{v}\cdot\mathrm{grad}_{\boldsymbol{x}}\mu_i + \mu_i\mathrm{div}_{\boldsymbol{x}}\boldsymbol{v} = \mathrm{div}_{\boldsymbol{x}}[\boldsymbol{D}_i\mathrm{grad}_{\boldsymbol{x}}\mu_i] + s_i,$$

The first two terms on the left-hand side are the material derivative of μ_i, which equals $\partial M_i/\partial t$ by definition of the pull-back. Using $\mathrm{div}_{\boldsymbol{x}}\boldsymbol{v} = \dot{J}/J$ the equation becomes

$$\frac{\partial M_i}{\partial t} + M_i\frac{\dot{J}}{J} = \mathrm{div}_{\boldsymbol{x}}[\boldsymbol{D}_i\mathrm{grad}_{\boldsymbol{x}}\mu_i] + s_i,$$

Applying the Piola identity to the diffusion term and using $\mathrm{grad}_{\boldsymbol{x}}\mu_i = \boldsymbol{F}^{-\mathrm{T}}\mathrm{GRAD}_{\boldsymbol{X}}M_i$, we get

$$\mathrm{div}_{\boldsymbol{x}}[\boldsymbol{D}_i\mathrm{grad}_{\boldsymbol{x}}\mu_i] = \frac{1}{J}\mathrm{DIV}_{\boldsymbol{X}}\left[J\boldsymbol{D}_{M_i}\mathrm{GRAD}_{\boldsymbol{X}}M_i\right]$$

where $\boldsymbol{D}_{M_i} = \boldsymbol{F}^{-1}\boldsymbol{D}_i\boldsymbol{F}^{-\mathrm{T}}$ is the effective material diffusion tensor for the species M_i, consistent with the definition provided for the cellular phase. We thus obtain the conservation law in the reference configuration:

$$\begin{aligned}
&\frac{\partial M_i(\boldsymbol{X},t)}{\partial t} + M_i\frac{\dot{J}}{J} = \frac{1}{J}\mathrm{DIV}_{\boldsymbol{X}}\left[J\boldsymbol{D}_{M_i}\mathrm{GRAD}_{\boldsymbol{X}}M_i\right]\\
&+S_i(\boldsymbol{X},t), \quad (12)
\end{aligned}$$

where the material source term $S_i(\boldsymbol{X},t) = s_i(\boldsymbol{\chi}(\boldsymbol{X},t),t)$ accounts for the net production or consumption rate transformed to the reference state. Substituting the Eulerian source term (7) and using $c = C/J$:

$$S_i(\boldsymbol{X},t) = -d_iM_i + \frac{\alpha_i}{J}C. \quad (13)$$

As in the Eulerian case, we need to define the reaction functions, R_{p}, R_{d}, S_i, as explicit functions of the cell density C and the external signals μ_i. Since some of these functions depend on the value of the signals at the current spatial position $\boldsymbol{x} = \boldsymbol{\chi}(\boldsymbol{X},t)$, we also need to compute the velocity of each RVE, which depends on the drag forces and cell movement driven by external taxis signals already mentioned for the discrete models. By integrating this velocity:

$$\boldsymbol{x}(\boldsymbol{X},t) = \boldsymbol{X} + \int_{\boldsymbol{0}}^{\boldsymbol{t}}\boldsymbol{V}(\boldsymbol{X},\tau)\,\mathrm{d}\tau, \quad (14)$$

we update the position $\boldsymbol{x} = \boldsymbol{\chi}(\boldsymbol{X},t)$, the deformation gradient $\boldsymbol{F}$, and the Jacobian J at each time step.

The resulting equations in both Eulerian and Lagrangian cases are usually solved by numerical methods, such as Finite Elements or Finite Volumes, which use interpolations or approximations of the solution in terms of several discrete values in space. This discretization transforms the original partial differential equations into a system of ordinary differential equations (ODEs) with respect to time, a structure like that of the discrete case, although with the flexibility provided by the huge amount of approximation methods available.

While Eulerian methods typically employ a fixed spatial mesh, Lagrangian procedures offer more flexibility in tracking material deformation through two main approaches: the Total Lagrangian formulation, where all variables are referred to the initial configuration at $t_0 = 0$; and the Updated Lagrangian procedure, where the reference configuration is

reset to the current state at the beginning of each time interval $[t, t+\Delta t]$. In the latter, the reference coordinates and state variables are incrementally updated ($\boldsymbol{X}_t \leftarrow \boldsymbol{X}_{t+\Delta t}$) after each successful time step.

As commented, the Lagrangian framework is widely used when one is interested in the history of individual elements [46, 47], and knows the initial position of each point. Consequently, it may be less suitable for problems where it is difficult to establish the initial configuration and/or the initial spatial distribution of each variable.

3. Modeling epigenetic evolution

Cells change their phenotypic state by epigenetic changes induced by their microenvironment. Epigenetic regulation shapes the long-term dynamics of cellular populations by enabling gradual and partially heritable modifications in gene expression without modifying the DNA sequence [48, 49]. Unlike genetic mutations, DNA methylation or histone modifications are reversible and can vary smoothly, generating a wide spectrum of cell behavior facilitating adaptation to environmental stresses, differentiate into specialized lineages, or acquire drug resistance [50, 51].

Over the last two decades, several families of computational models have been proposed to represent these processes. One first distinction is, again, between those that describe epigenetic dynamics as transitions between a discrete number of states and those that consider evolution in a continuous state space.

3.1. Modeling Cell Populations with a discrete number of phenotypes

In these models, each cell can adopt a finite number N of distinct phenotypes $\{\phi_1, \phi_2, \dots, \phi_N\}$, such as differentiated versus stem-like states or active versus repressed chromatin configurations. The dynamics of each cell phenotype can be formalized in any of the frameworks described in the previous section: namely ABMs or continuum equations in either a Lagrangian or Eulerian configuration. The ABM approach tracks the state E_k of each individual cell k. The probability of a state change during a time step Δt is given by:

$$P\left(E_k^{t+\Delta t} = j \mid E_k^t = i\right) = \kappa_{ij}\Delta t. \qquad (15)$$

This Markovian perspective is of course widely used as it allows for a tractable mathematical description of cell-state transitions and a direct interpretation of lineage-tracking data and single-cell plasticity. Alternatively, one can track the evolution of the population density $c_i(\boldsymbol{x}, t)$ for each phenotype ϕ_i at a fixed spatial location. The dynamics are then governed by a system of coupled flux balance equations following the ideas of Section 2:

$$\frac{\partial c_i}{\partial t} + \mathrm{div}_{\boldsymbol{x}}(\boldsymbol{v_i} c_i) = \mathrm{div}_{\boldsymbol{x}}\left(\boldsymbol{D}_{c,i}\mathrm{grad}_{\boldsymbol{x}} c_i\right)$$

$$+ \sum_{j\neq i}\left(\kappa_{ji} c_j - \kappa_{ij} c_i\right) + r_i c_i, \qquad (16)$$

where $\boldsymbol{v_i}$ is the velocity field of phenotype i, $D_{c,i}$ is the diffusion matrix and r_i represents the net growth (proliferation minus death). This Eulerian formulation can be mapped onto its Lagrangian counterpart via a pull-back operation, resulting in a material balance equation consistent with (8).

While the choice of framework determines how the collective dynamics is computed, the underlying biology is governed by the transition rates or probabilities between states, which represent the cellular response to multiscale stimuli. It is important to emphasize that this kinematic choice, whether formulated in the current or reference configuration, is a matter of mathematical representation for the bulk motion and does not dictate the underlying phenotypic dynamics. The general transition rate κ_{ij} from phenotype i to j (Eqs. 15, 16) allows us to categorize existing models based on which components are explicitly modeled and can be defined as a function of intrinsic stability, environmental cues (denoted from now on collectively as $\boldsymbol{\mu}$ in the spatial frame and $\boldsymbol{M}$ in the material frame), and cellular memory:

$$\kappa_{ij} = F_{ij}(G_{ij}, \mathcal{H}_{ij}(\boldsymbol{x}, t)), \qquad (17)$$

where G_{ij} represents the intrinsic stability of the phenotypic attractor (determined for example by the Gene Regulatory Network (GRN) architecture), and $\mathcal{H}_{ij}(\boldsymbol{x}, t)$ is the integrated signal history (memory), defined as:

$$\mathcal{H}_{ij}(\boldsymbol{x}, t) = \int_0^t W_{ij}(t-\tau)\boldsymbol{M}(\boldsymbol{\chi}^{-1}(\boldsymbol{x}, t), \tau)\, \mathrm{d}\tau, \qquad (18)$$

where W_{ij} is a history matrix kernel. It must be noted that to compute signal history it is unavoidable to resort to a material description of the stimuli, to track the history of cell trajectories. Note that if we neglect history dependence, that is, $W_{ij}(\tau) = \delta(\tau)I$, then we obtain a pure Eulerian expression for κ_{ij}:

$$\kappa_{ij} = F_{ij}(G_{ij}, \boldsymbol{\mu}(\boldsymbol{x}, t)) \qquad (19)$$

Instead of computing the history term $\mathcal{H}_{ij}$, an equivalent approach is to use internal variables. For a generic spatial vector $\boldsymbol{\xi}(\boldsymbol{x}, t)$ defined as $\boldsymbol{\xi} = \mathcal{H}(\boldsymbol{x}, t)$, using Leibniz derivation rule

$$\frac{\mathrm{D}\boldsymbol{\xi}}{\mathrm{D}t} = W(0)\boldsymbol{\mu}(\boldsymbol{x}, t)$$
$$+ \int_0^t \dot{W}(t-\tau)\, \boldsymbol{M}(\boldsymbol{\chi}^{-1}(\boldsymbol{x}, t), \tau)\, \mathrm{d}\tau. \qquad (20)$$

It is important to note that as the cell movement depends on epigenetic changes, the previous equation is a nonlinear PDE on $\boldsymbol{\xi}$ illustrating explicitly why the Eulerian approach is not the natural one for epigenetic changes tracking. Now let us define $\boldsymbol{\Xi}(\boldsymbol{X}, t) = \boldsymbol{\xi}(\boldsymbol{\chi}(\boldsymbol{X}, t), t)$. Then,

$$\left.\frac{\mathrm{D}\boldsymbol{\xi}}{\mathrm{D}t}\right|_{\boldsymbol{x}=\boldsymbol{\chi}(\boldsymbol{X},t)} = \frac{\partial \boldsymbol{\Xi}}{\partial t} \qquad (21)$$

This provides a material description of the internal epigenetic state. Next section explores this idea from the kinematic point of view. Evaluating Eq. (21) explicitly, the material evolution

equation for $\boldsymbol{\Xi}$ reads:

$$\frac{\partial \Xi(X,t)}{\partial t} = W(0)\boldsymbol{M}(\boldsymbol{X},t) + \int_0^t \dot{W}(t-\tau)\boldsymbol{M}(\boldsymbol{X},\tau)\,\mathrm{d}\tau \quad (22)$$

The literature on phenotypic transitions can be broadly categorized into two families based on the primary driver of the switch. On the one hand, models focused on intrinsic dynamics and stochasticity, rooted in GRNs, describe transitions because of molecular feedback loops that create bi-stability or multi-stability [52, 53]. In these frameworks, transitions are often triggered by molecular noise, allowing cells to jump between stable attractors in an epigenetic landscape. Later extensions have focused on cancer and reprogramming [54, 55] or, at the single cell level, for modeling the activity of chromatin regulators [56] using Markov processes. Alternatively, the population-level consequences of these transitions are often analyzed through Matrix Population Models (MPMs) [57, 58], focused on asymptotic behavior (by analyzing the spectral properties of the stable phenotype distribution towards which the population converges can be predicted) and applied to the study of how phenotypic plasticity (state) and other traits such as age affect population dynamics in plants [59] or invertebrates [58]. This perspective is further developed in mesoscopic frameworks where discrete traits are acquired through mutation probabilities [60], as well as in ODE models modeling processes such as drug resistance with sensitive and resistant compartments [61] or the epithelial-mesenchymal transition (EMT) where fixed transition rates are fitted to genomic data [62]. In this class of models, focused on intrinsic dynamics and stochasticity and thus exploring the interplay between the internal network architecture and noise, the transition rate can be set as $\kappa_{ij} \approx F(G_{ij}) + \zeta(t)$, where $\zeta(t)$ accounts for stochastic molecular noise. Transitions occur when stochastic fluctuations $\zeta(t)$ allow the system to overcome the potential barrier defined by G_{ij}. Note that this random term has not been included in the general definition of the transition rate in Eq. (17) to stay under the deterministic framework. Instead, the PDE framework captures the resulting mean-field transition rate, representing the collective probability of these stochastic jumps across the population.

On the other hand, a second family of models explicitly accounts for external stimuli—such as mechanical, biochemical, or social cues—as drivers of adaptation. In mechanobiology, for instance, volumetric strain and fluid shear stresses are modeled as governing factors for cell differentiation during bone fracture healing [63]. In mechanistic bone remodeling, mechanical strain regulates the local concentrations of signaling molecules such as RANKL, OPG, and TGF-β, which subsequently drive phenotypic changes [64, 65], while in wound healing, growth factors like PDGF and TGF-β act as the primary controllers of cellular state transitions. These external drivers often interact with cellular memory, as seen in hypoxia models where cells returning to normoxia do not revert to their original state but adopt persistent aggressive phenotypes [66, 67]. Another widespread application of this approach is the study of drug resistance, typically employing two-compartment models for sensitive and resistant populations with a transition dependent on drug exposure using ODEs [68, 69, 70] or stochastic models such as Markov branching processes that allow for random mutations [71, 72]. To bridge the gap toward continuous frameworks, these approaches could be extended by allowing an arbitrary number of phenotypes arranged along fitness axes [73]. Furthermore, this environmental influence extends to evolutionary game theory, where phenotypic transitions are modeled as frequency-dependent strategies. In these cases, the fitness and transition probability of a specific phenotype are conditioned by the composition of the surrounding population, capturing the competitive or cooperative nature of cellular ecosystems [74, 75].

In this family, the transition is driven by external cues, leading to $\kappa_{ij} \approx \mathcal{F}(\mu(\boldsymbol{x},t))$. In these cases, the internal biology G_{ij} is often treated as a constant threshold that μ_i must cross to trigger differentiation. In case of irreversible transitions [66, 67] the intrinsic term G_i acts as a one-way barrier with $\kappa_{ij} > 0$ and $\kappa_{ji} = 0$.

3.2. Modeling Cell Populations with Continuous Phenotype

A key challenge in modeling cellular adaptation and differentiation lies in representing the continuous evolution of internal state variables like chromatin organization, transcriptional activity, and metabolic configuration. In contrast to discrete models, continuous frameworks describe the epigenetic state of a cell by a set of real-valued variables. This approach aligns with the physical and biochemical nature of epigenetic modifications, which involve gradual addition and removal of biochemical markers.

Two main families of methods have been recently proposed within this framework: the first considers phenotype-structured models in which phenotypic variables are modeled as additional coordinates (independent variables), and the second in which phenotype is described by a set of dependent variables that evolve through local evolution laws without increasing the system's dimensionality.

3.2.1. Local Continuous Distribution of the Epigenetic Variables: Structured Models

Traditional continuum models of tissue dynamics operate solely in the physical space, $\Omega_{\boldsymbol{x}}$, describing how cell density or velocity evolves in time and position. However, now we want to consider that cells composing a certain RVE (or material point in continuous physics) may have different epigenetic states. If we want to track pointwise the evolution of this state distribution within a bounded set $\Omega_{\boldsymbol{\xi}}$, driven by epigenetic modifications or transcriptional reprogramming, we must extend the physical space to include additional dimensions that capture these new epigenetic coordinates.

The state of the system is then characterized by the evolution of each property like cell density $c(\boldsymbol{x},\boldsymbol{\xi},t)$, where $\boldsymbol{x} \in \Omega_{\boldsymbol{x}} \subset \mathbb{R}^3$ represents the physical position, and $\boldsymbol{\xi} \in \Omega_{\boldsymbol{\xi}} \subset \mathbb{R}^n$ represents the cell state [25, 76, 77]. The evolution of c is governed by a transport–reaction–diffusion equation that expresses the conservation of the cell number in the spatio-epigenetic extended

domain. Following (6), we can write again the Eulerian description as:

$$\frac{\partial c}{\partial t} + \mathrm{div}_{\boldsymbol{x}}(c\boldsymbol{v}_{\boldsymbol{x}}) + \mathrm{div}_{\boldsymbol{\xi}}(c\boldsymbol{v}_{\boldsymbol{\xi}}) = \mathrm{div}_{\boldsymbol{x}}(\boldsymbol{D}_{\boldsymbol{x}}\mathrm{grad}_{\boldsymbol{x}}c) + \mathrm{div}_{\boldsymbol{\xi}}(\boldsymbol{D}_{\boldsymbol{\xi}}\mathrm{grad}_{\boldsymbol{\xi}}c) + c(r_{\mathrm{p}} - r_{\mathrm{d}}) \quad (23)$$

where we have removed the dependence on each variable since it is stated in (2).

The reaction term $r_{\mathrm{p}} - r_{\mathrm{d}}$ represents the net production of cells at the spatial point $\boldsymbol{x}$, with state $\boldsymbol{\xi}$ and at time t, by proliferation or death. The flux $\boldsymbol{q}_{\mathrm{a},\boldsymbol{\xi}} = c\boldsymbol{v}_{\boldsymbol{\xi}}$ encodes the advection movement of cells in the epigenetic space, coming from transitions between epigenetic states induced by external signals. For instance, hypoxia or drug stress may induce a drift in $\boldsymbol{\xi}$ toward resistant or stem-like configurations [15]. The diffusion term $\mathrm{div}_{\boldsymbol{\xi}}(\boldsymbol{D}_{\boldsymbol{\xi}}\,\mathrm{grad}_{\boldsymbol{\xi}}\,c)$ captures stochastic gene-regulatory fluctuations in the epigenetic state [21, 22], producing, for example, natural decay driving cells back towards baseline states in the absence of external signals. Boundary conditions at the edges of $\Omega_{\boldsymbol{\xi}}$ limit the epigenetic transitions, effectively constraining the admissible phenotypic range. Therefore, the resulting cell distribution $c(\boldsymbol{x},\boldsymbol{\xi},t)$ describes not only how cells move in the physical space, but also how their identity is distributed in the epigenetic landscape. Eq. (23) can be written using a compact notation as:

$$\frac{\partial c}{\partial t} + \mathrm{div}_{\boldsymbol{y}}(c\boldsymbol{v}_{\boldsymbol{y}}) = \mathrm{div}_{\boldsymbol{y}}(\boldsymbol{D}_{\boldsymbol{y}}\mathrm{grad}_{\boldsymbol{y}}c) + c(r_{\mathrm{p}} - r_{\mathrm{d}}) \quad (24)$$

with $\boldsymbol{v}_{\boldsymbol{y}} = (\boldsymbol{v}_{\boldsymbol{x}}, \boldsymbol{v}_{\boldsymbol{\xi}})$ and $\boldsymbol{D}_{\boldsymbol{y}} = \mathrm{diag}(\boldsymbol{D}_{\boldsymbol{x}}, \boldsymbol{D}_{\boldsymbol{\xi}})$. The distribution of cells in the real spatial domain, $\rho(\boldsymbol{x},t)$ can be recovered by:

$$\rho(\boldsymbol{x},t) = \int_{\Omega_{\boldsymbol{\xi}}} c(\boldsymbol{x},\boldsymbol{\xi},t)\,\mathrm{d}\boldsymbol{\xi},$$

To analyze history-dependent behavior and phenomena such as cell conditioning, we may transition from the Eulerian description presented above to its Lagrangian counterpart. We define the material coordinate $\boldsymbol{Y} = (\boldsymbol{X},\boldsymbol{\Xi})$, representing the initial position and epigenetic state of a cell cohort at t = 0. The current configuration $\boldsymbol{y} = (\boldsymbol{x},\boldsymbol{\xi})$ is determined by the motion mapping $\boldsymbol{y} = \boldsymbol{\chi}(\boldsymbol{Y},t)$, which is obtained by integrating the coupled system of ordinary differential equations:

$$\frac{\mathrm{d}\boldsymbol{x}}{\mathrm{d}t} = \boldsymbol{v}_{\boldsymbol{x}}(\boldsymbol{x},\boldsymbol{\xi},t), \quad \frac{\mathrm{d}\boldsymbol{\xi}}{\mathrm{d}t} = \boldsymbol{v}_{\boldsymbol{\xi}}(\boldsymbol{x},\boldsymbol{\xi},t) \quad (25)$$

subject to the initial conditions $\boldsymbol{x}(\boldsymbol{X},0) = \boldsymbol{X}$ and $\boldsymbol{\xi}(\boldsymbol{\Xi},0) = \boldsymbol{\Xi}$. Note that while the velocities $\boldsymbol{v}_{\boldsymbol{x}}$ and $\boldsymbol{v}_{\boldsymbol{\xi}}$ depend on the current state $(\boldsymbol{x},\boldsymbol{\xi})$ to reflect local microenvironmental stimuli (e.g., chemotactic gradients or stress-induced reprogramming), the resulting trajectories are uniquely identified by their material labels $(\boldsymbol{X},\boldsymbol{\Xi})$.

In this framework, the material density $C(\boldsymbol{Y},t)$ represents the number of cells per unit of initial spatio-epigenetic volume. It is related to the spatial density c through the Jacobian $J = \det(\boldsymbol{F}_{\boldsymbol{Y}})$, such that $C(\boldsymbol{Y},t) = Jc(\boldsymbol{\chi}(\boldsymbol{Y},t),t)$. We can obtain the material analogous of (11) from Eq. (24). Applying the Piola identity in the extended space, $J\,\mathrm{div}_{\boldsymbol{y}}\boldsymbol{b} = \mathrm{DIV}_{\boldsymbol{Y}}(J\boldsymbol{F}_{\boldsymbol{Y}}^{-1}\boldsymbol{b})$, together with the pull-back of the extended spatial gradient, $\mathrm{grad}_{\boldsymbol{y}}\,f = \boldsymbol{F}_{\boldsymbol{Y}}^{-\mathrm{T}}\,\mathrm{GRAD}_{\boldsymbol{Y}}\,f$, and the block-diagonal structure of the spatial diffusion tensor $\boldsymbol{D}_{\boldsymbol{y}}$ to obtain:

$$\frac{\partial C(\boldsymbol{Y},t)}{\partial t} = \mathrm{DIV}_{\boldsymbol{Y}}\left(J\boldsymbol{D}_{\boldsymbol{Y}}\mathrm{GRAD}_{\boldsymbol{Y}}\left(\frac{C}{J}\right)\right) + CR(\boldsymbol{Y},t), \quad (26)$$

where $R = R_{\mathrm{p}} - R_{\mathrm{d}}$ is the net growth rate evaluated along the trajectory and the effective material diffusion tensor in the extended space is:

$$\boldsymbol{D}_{\boldsymbol{Y}} = \boldsymbol{F}_{\boldsymbol{Y}}^{-1}\boldsymbol{D}_{\boldsymbol{y}}\boldsymbol{F}_{\boldsymbol{Y}}^{-\mathrm{T}}$$

It is important to note that even though $\boldsymbol{D}_{\boldsymbol{y}}$ is block-diagonal, $\boldsymbol{D}_{\boldsymbol{Y}}$ is not in general, since the off-diagonal blocks of $\boldsymbol{F}_{\boldsymbol{Y}}$ introduce cross-coupling terms between spatial and epigenetic directions. These blocks are:

$$\frac{\partial \boldsymbol{x}}{\partial \boldsymbol{\Xi}}, \quad \frac{\partial \boldsymbol{\xi}}{\partial \boldsymbol{X}}$$

which are generically non-zero: the first encodes how the current spatial position of a cell depends on its initial epigenetic state (cells with different phenotypes migrate differently), and the second encodes how the current epigenetic state depends on the initial spatial position (cells in different microenvironments undergo different epigenetic evolution). Only when both blocks vanish does $\boldsymbol{F}_{\boldsymbol{Y}}$ become block-diagonal, J factorizes *as* $J_{\boldsymbol{X}}J_{\boldsymbol{\Xi}}$, and Eq. (26) reduces to

$$\frac{\partial C(\boldsymbol{Y},t)}{\partial t} = \mathrm{DIV}_{\boldsymbol{X}}\left(J_{\boldsymbol{X}}\boldsymbol{D}_{\boldsymbol{X}}\mathrm{GRAD}_{\boldsymbol{X}}\left(\frac{C}{J_{\boldsymbol{X}}}\right)\right) + \mathrm{DIV}_{\boldsymbol{\Xi}}\left(J_{\boldsymbol{\Xi}}\boldsymbol{D}_{\boldsymbol{\Xi}}\mathrm{GRAD}_{\boldsymbol{\Xi}}\left(\frac{C}{J_{\boldsymbol{\Xi}}}\right)\right) + CR(\boldsymbol{Y},t), \quad (27)$$

A fundamental advantage of this Lagrangian approach is that the complex advection terms from the Eulerian description—namely $\mathrm{div}_{\boldsymbol{x}}(c\boldsymbol{v}_{\boldsymbol{x}})$ and $\mathrm{div}_{\boldsymbol{\xi}}(c\boldsymbol{v}_{\boldsymbol{\xi}})$—are implicitly handled by the trajectory mapping $\boldsymbol{\chi}$. In the material frame, the coordinate system moves with the cell cohort and thus, the flow of cells through the epigenetic landscape is embedded in the evolution of $\boldsymbol{y}(t)$. Moreover, this formulation effectively preserves the identity of cell lineages. This path-dependency is critical for modeling how prior environmental exposure determines the current adaptive capacity of tumor cells.

The phenotype-structured framework has been extensively applied to capture clonal selection and population heterogeneity in cancer evolution. Early foundational models in this area primarily focused on selection-driven dynamics, where phenotypic drift is neglected ($\boldsymbol{v}_{\boldsymbol{\xi}} = \boldsymbol{0}$). This is classical mean field theory obtained from random fluctuations of epigenetic noise. In these cases, the evolution of $c(\boldsymbol{x},\boldsymbol{\xi},t)$

is governed by differential proliferation and migration rates along the phenotypic dimensions and random mutations, modeled through diffusion in $\Omega_{\boldsymbol{\xi}}$. This approach has been applied to study the interplay between cells and oxygen levels [78, 16], the go or grow behavior of tumor cells [79] or drug resistance [76, 80]. More recently, the inclusion of an advective phenotypic drift ($\boldsymbol{v}_{\boldsymbol{\xi}} \neq \mathbf{0}$) has allowed to model microenvironment-driven plasticity, by adding a drift as in Fokker-Planck equation. Examples include [25, 15], where cells are driven to stem-like phenotypes when exposed to hypoxia (see some results in Figure 1), or [81], where the Epithelial-to-Mesenchymal transition is modeled with phenotype changes driven by the density of the ECM. Additionally, in [82] the drift is caused by an epigenetic drug.

Besides cancer, there are other applications of this approach ranging from general formulations under the prism of evolutionary biology for populations under fluctuating environments [81] to particular examples of bacterial persistence under antibiotic stress, developmental differentiation or immune adaptation. The reader is referred to [83] for a more thorough review.

This extra-dimension formalism bridges the gap between microscopic stochastic models of molecular regulation and macroscopic tissue-scale descriptions and is a versatile tool for representing continuous phenotypic plasticity in cell populations.

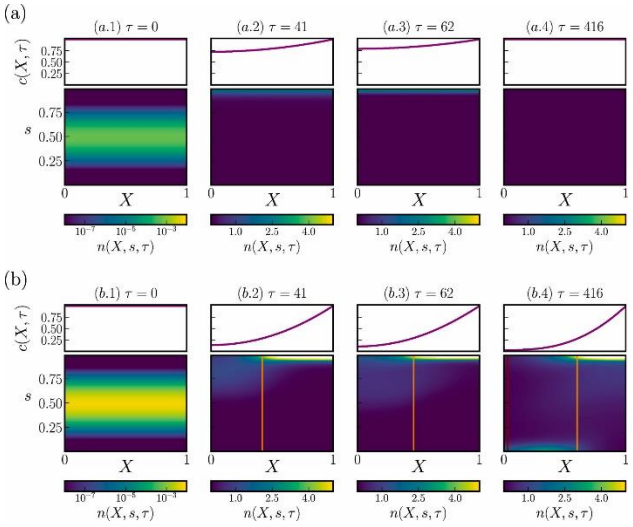

Fig 1: Results of cell evolution in the extended spatial-phenotypic space using a structured model. The first and second rows respectively reproduce two cases, and each column corresponds to a time step of cell evolution along the phenotypic dimension *s* (where *s = 0* corresponds to differentiated cells and *s = 1* to cancer stem cells) and space ***X***. Reproduced from [15].

3.2.2. The Internal Variable Approach in Continuous Epigenetic Evolution

Inspired by the fundamentals of internal state theory in control theory [84] and continuum mechanics [85], an alternative approach to the ones described above was presented and applied in the work of Pérez-Aliacar and colleagues [13, 14] using internal variables to describe the phenotypic state of cells.

The internal variable formalism originates from non-equilibrium thermodynamics, where it represents hidden degrees of freedom that store history-dependent information [86, 87]. In the biological context, the internal variables represent the epigenetic state, encoding memory of past conditions such as hypoxia or therapy exposure. Therefore, we consider a finite dimensional spatial continuous distribution of epigenetic states, with values at each spatial point $\boldsymbol{x}$ and time t, as a real-valued finite-dimensional vector $\boldsymbol{\xi}$. These internal variables are considered as properties that are carried by each cell RVE (each material point). They change along their trajectory under environmental stimuli, so their evolution is mathematically defined by an evolution equation like that of cellular concentration. Inheritance at division—full, partial, or noisy—can be represented by appropriate rules to conserve or dilute epigenetic memory across generations, providing a minimal mathematical expression for epigenetic heritability in proliferating populations [14].

As the general framework formulated in [13], this approach considers *m* cell populations characterized by their densities $c^k(\boldsymbol{x}, t)$. Each population k is endowed with d_k specific epigenetic internal variables, $\xi_i^k(\boldsymbol{x}, t) \in \Gamma_i^k \subset \mathbb{R}$ $(i = 1, \dots, d_k)$, representing the epigenetic accumulation per unit cell within an RVE. Finally, the environment is described by n chemical species acting as signals, with mass concentrations $\mu_j(\boldsymbol{x}, t)$ $(j = 1, \dots, n)$.

The evolution of these variables is derived from conservation laws [13]. The conservation equation for the epigenetic state per unit volume, $c^k \xi_i^k$, in the absence of a diffusive flux for the epigenetic state (consistent with the assumption that epigenetic transport occurs solely through cell convection), reads:

$$\frac{\partial (c^k \xi_i^k)}{\partial t} + \operatorname{div}_{\boldsymbol{x}}\left(\xi_i^k \boldsymbol{q}^k\right) = c^k f_i^k, \qquad (28)$$

where $\boldsymbol{q}^k = c^k \boldsymbol{v} + \boldsymbol{q}_{\mathrm{d}}^k$ is the total cell flux (advective plus diffusive) and f_i^k is the epigenetic source term per unit cell. Expanding (28) using the product rule, substituting into (28) and collecting the terms multiplying ξ_i^k:

$$\xi_i^k \left(\frac{\partial c^k}{\partial t} + \operatorname{div}_{\boldsymbol{x}} \boldsymbol{q}^k\right) + c^k \frac{\partial \xi_i^k}{\partial t} + \boldsymbol{q}^k \cdot \operatorname{grad}_{\boldsymbol{x}} \xi_i^k = c^k f_i^k,$$

The bracketed term is recognized as the left-hand side of the cell conservation equation (4):

$$\frac{\partial c^k}{\partial t} + \operatorname{div}_{\boldsymbol{x}} \boldsymbol{q}^k = r^k c^k,$$

where $r^k = r_{\mathrm{p}}^k - r_{\mathrm{d}}^k$ is the net proliferation rate. Substituting:

$$r^k c^k \xi_i^k + c^k \frac{\partial \xi_i^k}{\partial t} + \boldsymbol{q}^k \cdot \operatorname{grad}_{\boldsymbol{x}} \xi_i^k = c^k f_i^k.$$

Solving for $\partial \xi_i^k / \partial t$ and dividing through by c^k yields the evolution equation for the epigenetic variable:

$$\frac{\partial \xi_i^k}{\partial t} = \underbrace{f_i^k}_{\text{source}} - \underbrace{r^k \xi_i^k}_{\text{net balance}} \underbrace{- \frac{1}{c^k} \boldsymbol{q}^k \cdot \operatorname{grad}_{\boldsymbol{x}} \xi_i^k}_{\text{convection}}. \qquad (29)$$

The convection term ensures consistency within the Eulerian framework as the state is transported with the cellular movement. Finally, f_i^k is the source term, expressed as:

$$f_i^k = \underbrace{\omega_i^k}_{\text{acquisition}} - \underbrace{\lambda_i^k \xi_i^k}_{\text{repair}} + \underbrace{\beta_i^k r_{\mathrm{p}}^k \xi_i^k}_{\text{inheritance}} - \underbrace{r_{\mathrm{d}}^k \xi_i^k}_{\text{cell death}}, \quad (30)$$

where $\omega_i^k = p_i^k(\boldsymbol{\mu}(\boldsymbol{x},t), \boldsymbol{\xi}(\boldsymbol{x},t))$ models the acquisition of epigenetic changes, that might be induced by a combination of external stimuli, their rates and gradients and the current level of the internal variables themselves, which allows to model cell adaptation as a response to environmental changes; λ_i^k is a decay coefficient representing spontaneous repair mechanisms. The third term accounts for phenotypic inheritance during cell division (governed by the growth rate r_{p}); here, β_i^k represents the fraction of the phenotypic state inherited by daughter cells. In this regard, the term is proportional to the growth rate in cells r_{p} through the coefficient $\beta_i^k \in [0,1]$ that regulates inheritance in such a way that when $\beta_i^k = 1$ daughter cells inherit the phenotypic state of their progenitor, whereas when $\beta_i^k < 1$, only a percentage of daughter cells inherits the state of their parents. Finally, the fourth term incorporates the reduction of epigenetic charge due to cell death and therefore it is proportional to death rate r_{d}. By plugging Eq. (30) in Eq. (29), we obtain the final expression for the evolution of the internal variable

$$\frac{\partial \xi_i^k}{\partial t} = \omega_i^k - \lambda_i^k \xi_i^k + (\beta_i^k - 1) r_{\mathrm{p}}^k \xi_i^k - \frac{1}{c^k} \boldsymbol{q}^k \cdot \mathrm{grad}_{\boldsymbol{x}} \xi_i^k. \quad (31)$$

The governing equations for cell populations and species are those detailed in the previous section, with the nuance that now the internal variables $\xi^k = (\xi_1^k, .., \xi_{d_k}^k)$ modulate the populations' behavior by influencing its flux $\boldsymbol{q}^k$, growth and death rates, r_{p}^k and r_{d}^k, in the case of cells, and consumption/production α_i in the case of species. That is, the internal variables representing the phenotypic state modulate the populations' behavior thereby closing the coupling between the environment and cellular response.

Finally, to accurately capture complex, biological processes in which history-dependence is sought to be tracked individually, a Lagrangian formulation is often better suited than its Eulerian counterpart. In this framework, we track individual RVEs as material points, integrating the environmental stimuli they experience along their specific trajectories.

As in the previous section, let $\boldsymbol{X}$ denote the reference (initial) position of a material RVE at $t = 0$, and $\boldsymbol{x} = \boldsymbol{\chi}(\boldsymbol{X}, t)$ its current position at time t, with the mapping both configurations obtained by integrating the material velocity $\boldsymbol{V}(\boldsymbol{X}, t)$, determined by the local microenvironmental signals and the current phenotypic state of the RVE.

Let $\Xi_i^k(\boldsymbol{X}, t) = \xi_i^k(\boldsymbol{\chi}(\boldsymbol{X}, t), t)$ represent the epigenetic internal variables associated with the material point $\boldsymbol{X}$ per unit cell. By moving with the cellular RVE, the explicit convective term vanishes, and the conservation law (28) for the epigenetic state can be rewritten in its material form. First, we apply the pull-back of the three fields involved. The spatial gradient of ξ_i^k transforms via the inverse transposed deformation gradient:

$$\mathrm{grad}_{\boldsymbol{x}} \xi_i^k = \boldsymbol{F}^{-\mathrm{T}} \mathrm{GRAD}_{\boldsymbol{X}} \Xi_i^k.$$

The cell concentration satisfies $C^k = J c^k$, and the diffusive cell flux transforms according to the Nanson formula for vectors,

$$\boldsymbol{Q}_{\mathrm{d}}^k = J \boldsymbol{F}^{-1} \boldsymbol{q}_{\mathrm{d}}^k \Rightarrow \boldsymbol{q}_{\mathrm{d}}^k = \frac{1}{J} \boldsymbol{F} \boldsymbol{Q}_{\mathrm{d}}^k.$$

Combining these three relations:

$$\frac{\boldsymbol{q}_{\mathrm{d}}^k}{c^k} \cdot \mathrm{grad}_{\boldsymbol{x}} \xi_i^k = \frac{J}{c^k} \frac{1}{J} \boldsymbol{F} \boldsymbol{Q}_{\mathrm{d}}^k \cdot \boldsymbol{F}^{-\mathrm{T}} \mathrm{GRAD}_{\boldsymbol{X}} \Xi_i^k = \frac{1}{c^k} (\boldsymbol{F} \boldsymbol{Q}_{\mathrm{d}}^k) \cdot (\boldsymbol{F}^{-\mathrm{T}} \mathrm{GRAD}_{\boldsymbol{X}} \Xi_i^k).$$

Expanding the scalar product and using $\boldsymbol{F}^{\mathrm{T}} \boldsymbol{F}^{-\mathrm{T}} = \mathrm{I}$:

$$(\boldsymbol{F} \boldsymbol{Q}_{\mathrm{d}}^k) \cdot (\boldsymbol{F}^{-\mathrm{T}} \mathrm{GRAD}_{\boldsymbol{X}} \Xi_i^k) = \boldsymbol{Q}_{\mathrm{d}}^k \cdot \mathrm{GRAD}_{\boldsymbol{X}} \Xi_i^k$$

Therefore:

$$\frac{\boldsymbol{q}_{\mathrm{d}}^k}{c^k} \cdot \mathrm{grad}_{\boldsymbol{x}} \xi_i^k = \frac{1}{c^k} \boldsymbol{Q}_{\mathrm{d}}^k \cdot \mathrm{GRAD}_{\boldsymbol{X}} \Xi_i^k$$

Substituting this result into the material form of (29), we obtain the exact Lagrangian evolution equation for the epigenetic variable:

$$\frac{\partial \Xi_i^k}{\partial t} = F_i^k - \frac{1}{c^k} \boldsymbol{Q}_{\mathrm{d}}^k \cdot \mathrm{GRAD}_{\boldsymbol{X}} \Xi_i^k. \quad (32)$$

where $F_i^k(\boldsymbol{X}, t) = f_i^k(\boldsymbol{\chi}(\boldsymbol{X}, t), t) - R^k(\boldsymbol{X}, t) \Xi_i^k(\boldsymbol{X}, t)$ is the material source term. The advective part of the convective term, $\boldsymbol{v} \cdot \mathrm{grad}_{\boldsymbol{x}} \xi_i^k$, is absorbed into the material time derivative and thus disappears in the Lagrangian frame. However, the residual transport term $\frac{1}{c^k} \boldsymbol{Q}_{\mathrm{d}}^k \cdot \mathrm{GRAD}_{\boldsymbol{X}} \Xi_i^k$ persists and accounts for the redistribution of the epigenetic state driven by the random (diffusive) motion of cells relative to the mean velocity field $\boldsymbol{v}$, and vanishes only if this diffusive cell flux is negligible. Eq. (32) is analogous to Eq. (22). Note that, unlike the formulation for cellular concentration C, the Jacobian $J = \det \boldsymbol{F}$ does not appear explicitly in the diffusion term for Ξ_i^k. This is because Ξ_i^k is defined as an intensive property per unit cell, making its transport independent of volumetric dilution. The term F_i^k is the material source term, which tracks the net rate of phenotypic changes per unit cell as it navigates the domain:

$$F_i^k = \Omega_i^k - \Lambda_i^k \Xi_i^k + (\beta_i^k - 1) R_{\mathrm{p}} \Xi_i^k \quad (33)$$

where now $\Omega_i^k = P_i^k(\boldsymbol{M}(\boldsymbol{X}, t), \boldsymbol{\Xi}(\boldsymbol{X}, t))$. In this setting, the internal variables act as a biological memory, accumulating the effects of past exposure to stressors such as hypoxia or drug concentrations. This Lagrangian framework bridges the

gap between discrete cellular histories and continuum tissue mechanics, providing a robust pathway to track the emergence of drug-resistant niches.

In [13], this general framework (in its Eulerian formulation) is particularized to the study of glioblastoma (GBM) adaptation to hypoxia through several simplifications, i.e., there is only one cell type and one epigenetic variable, that evolves depending on hypoxia exposure without considering random mutations. As an illustration, figure 2 reproduces cell and phenotypic state evolution for a particular case. The internal variable approach proves its ability to replicate *in vitro* data of drug resistance in GBM spheroids [14] in this case using an ODE model with again one phenotypic variable, demonstrating that macroscopic observables (growth curves, viability, rebound after drug holidays) can be reproduced with a unique point-wise value of the phenotypic variable.

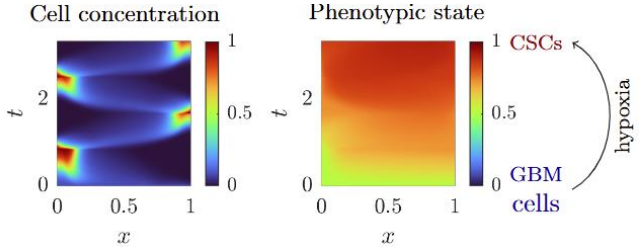

Fig 2: Cell and phenotypic state evolution with the internal variable approach. Example of GBM cells under an in silico cyclic hypoxia experiment, where cells migrate towards the oxygenated area while undergoing phenotypic changes, ranging from GBM differentiated cells to Cancer Stem Cells (CSCs) due to hypoxia exposure. Reproduced from [13].

To close this section, Table 1 summarizes the main features of the two families of models discussed for modeling phenotype as a continuum variable.

4. Discussion. Comparison and Conceptual Integration of the Different Models

The choice between these paradigms (discrete versus continuous, structural versus internal variables, and Eulerian versus Lagrangian) depends on the data available, the scale, and the question of interest among other factors. In the following, we highlight the main characteristics of each approach versus its alternative, identify the main pros and cons of each of them for specific applications and establish the connections between them.

4.1. Discrete Versus Continuous Cell Models

From all the discussed in previous sections, it becomes clear that discrete models are attractive due to their simplicity and biological interpretability. They provide a natural description of the system, with real stimuli and responses, catching nontrivial dynamic behaviors such as hysteresis, multistability, and oscillations [21]. They also allow direct correspondence with experimentally observed phenotypic categories, and their parameters—transition rates, proliferation rates, or death rates—can be estimated from population-level data. Since they work at the individual scale, they allow to analyze how local interactions give rise to global behavior, thus capturing emergent phenomena at the population-level [88]. Moreover, they inherently incorporate stochastic phenomena, allowing to control and analyze predictions uncertainty [89]. Finally, they have a modular structure and are much flexible, allowing to easily introduce new agents or rules, without modifying the entire model. However, they have a high computational cost due to their combinatoric nature when considering cell interactions. This makes them prohibitive for large numbers of cells as happens when solving tissue-scale domains. They also have many parameters, which makes it difficult parameter identifiability [90] making the fitting task extremely complicated [91]. Finally, they tend to be more dependent on their implementation than continuous approaches [92].

Conversely, the continuum formalism provides direct access to distributions and fluxes that can be compared with experimental histograms obtained from flow cytometry, single-cell sequencing, or imaging. Furthermore, they naturally accommodate heterogeneous environments and easily show how local environmental variables (e.g. oxygen, drugs, nutrients) influence on the drift and diffusion coefficients, leading to spatially dependent adaptation patterns [93, 76]. They also permit an easy derivation of macroscopic integral quantities—such as mean phenotype, total cell number, and spatial fluxes over surfaces and, therefore, an easy coupling with continuum models of nutrient diffusion, mechanical stress, and therapy delivery. However, continuum formulations do not permit to distinguish between cells located at the same point with distinct properties if they are not considered as different entities, which implies an increase in the number of variables to model. New hybrid models are proposed with the aim of combining the best of both worlds. For example, ABMs may be used to inform the parameters and closures of continuum equations [94, 95], while continuum models can provide averaged fields that guide stochastic simulations [96, 97].

Alternatively, some frameworks integrate discrete agents that interact with continuum fields of nutrients, chemical signals, or mechanical stress, providing a flexible multiscale framework [18, 39]. Finally, in other hybrid approaches, continuous PDEs describe the global evolution of cell distributions, while discrete stochastic models capture rare switching events or lineage tracking [55, 22].

Correlating the equations and parameters of these two approaches is essential for building consistent, multiscale models of cell populations, and to facilitate the integration with data and between them. Many works such as [98, 99, 100, 101, 102, 103] derive a complete set of relationships between the parameters of a class of ABMs, incorporating cellular proliferation and death, as well as random and directed migration, with continuum models that describe the combined effects of reaction, convection, and diffusion (see Figure 3 for an example of the equivalence between ABMs and continuum models in GBM cultures in microfluidic devices).

Regarding the modeling of phenotypic plasticity, structured continuous epigenetic models have recently been derived from ABMs by taking the continuum limit, including the dependence of migration and proliferation on the cell phenotypic state [105, 82, 77].

Table 1: Comparative analysis of continuum phenotypic modeling frameworks: Phenotype-structured models and Internal variables.

Feature	Phenotype-Structured	Internal Variables
Mathematical Basis	PDEs (Adv.-Diffusion) in extended space $(\boldsymbol{x}, \boldsymbol{\xi})$	PDEs in real space $\boldsymbol{x}$ for cells and phenotype $\boldsymbol{\xi}$.
Phenotype ($\boldsymbol{\xi}$)	Continuous independent variable.	Property attached to the point and convected with cells.
Variables describing phenotype	Infinite (continuous distribution).	Finite (one value per internal variable).
Computational Cost	High: Requires mesh in $n+1$ dimensions.	Moderate: Standard mesh; extra DOF per node.
Cell History	Difficult to track in Eulerian grids (mixing).	More natural translation to a Lagrangian frame.

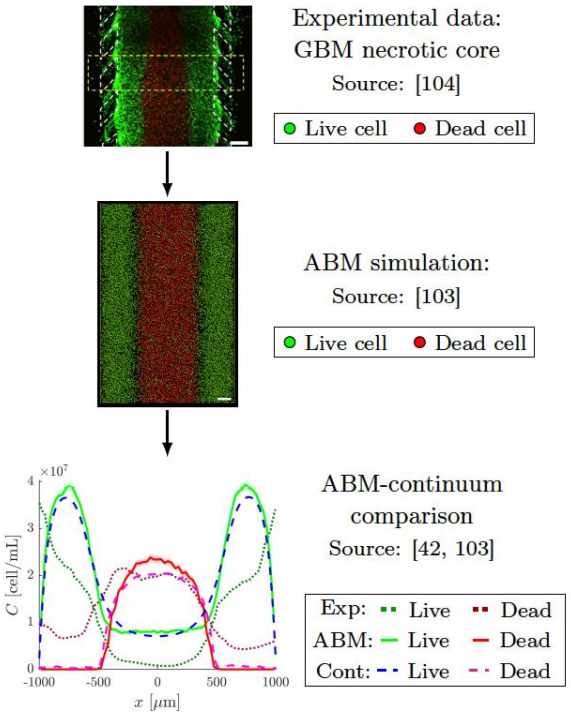

Fig 3: Equivalence between discrete and continuum models. Case example of the simulation of the formation of a necrotic core in glioblastoma (GBM) inside a microfluidic devices. Images reproduced from [104, 103, 42].

4.2. Structural Continuous Versus Internal Variables to Model Epigenetic Transitions

Discrete models concentrate each differential behavior in one specific phenotype. This may lead to a large amount of different phenotypes, or alternatively, if this number is maintained small, we may be forced to homogenize phenotypic differences that can be of interest in particular situations. This approach inherently assumes discontinuous boundaries between cell states, neglecting the continuous spectrum of transcriptional configurations that modern single-cell data reveal [7, 106].

To capture this gradual and history-dependent landscape without artificial discretization, frameworks must represent phenotypic evolution as a continuous process coupled with environmental factors. This is typically achieved through two main paradigms: extra-dimensional structural models [81, 25] and the internal variables approach [13, 14].

The primary advantage of extra-dimensional models lies in their completeness. They provide a detailed population-level description of evolving heterogeneity, capturing full phenotypic distributions and explaining emergent phenomena such as bimodality or selection-driven drift. This facilitates direct comparison with single-cell datasets, which increasingly report distributions rather than population averages. However, these models face significant hurdles; tracking individual cell trajectories —essential for modeling memory or hysteresis— is difficult unless further state variables are introduced. Furthermore, parameter identification is challenging, as the functional forms of $\boldsymbol{v}_{\xi}$, $\boldsymbol{D}_{\xi}$, and $R(c, \boldsymbol{x}, \boldsymbol{\xi}, t)$ are rarely directly measurable. Finally, they are computationally expensive, as the discretization of the extended domain is constrained by the curse of dimensionality as phenotypic dimensions increase.

In contrast, the internal variables (IV) framework describes the mean evolution of the epigenetic state through a set of dependent variables and their evolution equations. Relative to the extra-dimensional family, the IV method offers several practical advantages: it naturally accommodates long-term memory effects, aligns with typical experimental regimes where low-order statistics are more readily available than full high-dimensional distributions, and remains modular. Adding new biological dimensions, such as a DNA-damage response state, augments the constitutive set without an exponential explosion in degrees of freedom, facilitating 3D tissue-scale studies coupled with nutrient diffusion and mechanics. The principal limitation of this method is its inability to resolve distributional shapes, such as tails or multimodality; when such features are critical, the model must be enriched with higher-order moments or reverted to a continuous distribution. Additionally, reducing stochastic inheritance and division noise to scalar variables is a pragmatic but significant simplification of epigenetic variability.

The relationship between both approaches is clarified by interpreting the IV framework as a discretized projection of the structural model. If a continuous epigenetic coordinate follows a predefined probability density function (PDF), the set of moments defining that PDF can be identified as a finite set of internal variables whose evolution can be derived. This moment closure provides a natural bridge between both formalisms. Indeed, it is possible to define any finite-dimensional vector by means of a functional acting on a structured function f, $\lambda = \mathcal{F}(f)$ (note that statistical moments are particular cases). Under this setting, the evolution equation for λ is obtained immediately via the Gateaux derivative $\dot{\lambda} = D(f(\cdot,t);\, \partial_t f(\cdot,t))$. For instance, for models with the epigenetic state ξ as an independent variable and linear functionals (such as moments or collocations), $\mathcal{F}[c](\boldsymbol{x},t) = \int_{\Omega_{\xi}} K(\boldsymbol{x},\boldsymbol{\xi}) c(\boldsymbol{x},\boldsymbol{\xi},t)\, \mathrm{d}\boldsymbol{\xi}$, the Gateaux derivative is the functional itself. Thus, the evolution of the dependent variable $\boldsymbol{\xi}'$ is given by

$$\frac{\partial \xi'}{\partial t} = \int_{\Omega_\xi} K(\boldsymbol{x}, \boldsymbol{\xi}) \frac{\partial c}{\partial t}(\boldsymbol{x}, \boldsymbol{\xi}, t)\, \mathrm{d}\boldsymbol{\xi}.$$

In particular, for specific PDEs that have the closure property for parametric families (e.g. exponential families), the evolution of f is strictly determined by the evolution of its defining parameters. This usually happens for linear evolution equations.

The computational efficiency of the IV approach is particularly evident in large-scale simulations: for a 3D hexahedral grid of N^3 elements, a structural model with n_ξ dimensions (each discretized with m points) requires solving a system of $N^3 \times m^{n_\xi}$ equations, whereas the IV approach solves only N^3 spatial equations, followed by the efficient, parallelizable computation of $(8 \times n_\xi)N^3$ internal variables. Moreover, the Lagrangian formulation of the internal variable approach is usually simpler since knowing the initial distribution of epigenetic values at each spatial point is more complex. Conversely, integrating cell concentrations over the epigenetic coordinates and invoking suitable closures yields the evolution of the internal variables. This equivalence clarifies why internal variables often suffice in practice—especially when distributions remain narrow—and why extra-dimensional models become valuable when the distribution itself is the object of inference or control.

Figure 4 summarizes the main families discussed in this work to model epigenetic state, providing intuition to how they can be related to one another.

4.3. Eulerian Versus Lagrangian Formalisms to Model Continuous Cell Processes

Although the two continuous descriptions are equivalent mathematically, they emphasize different aspects. The analogy with continuum mechanics provides conceptual clarity. In fluid dynamics, the Eulerian formulation observes the flow field at fixed spatial locations, while the Lagrangian formulation follows individual fluid parcels. Thus, the Eulerian approach captures the collective evolution of fields, enabling the analysis of global patterns, gradients, and fluxes. The Lagrangian formulation emphasizes the individual perspective, making it natural to model memory effects, and track the evolution of history-dependent internal variables. It is worth mentioning that in Eulerian approaches even if we take phenotypic plasticity into account, it is impossible to assign to a cell at a given RVE its history of perceived stimuli without solving before the transport equations, so a mechanistic approach for epigenetic transitions is harder.

The following list of the differences between these two approximations highlights their main pros and cons. First, in the Lagrangian formulation, it is easier:

1. To ensure the conservation of quantities that affect a cellular RVE (e.g., concentration if there is no proliferation or death, and phenotype if there are no changes in it in a certain volume, although it may have changes per cell).
2. To track the evolution of a group of cells defined by any initial characteristic, such as their phenotype (tracking trajectories).
3. To track interfaces (e.g., cell groups with different initial phenotype).
4. To consider "mixing" problems (phenotypes close to each other but with different behavior).
5. To establish the relationship with discrete cell or discrete phenotype models.
6. To consider memory, hysteresis or hereditary effects.
7. To know the variations in phenotype over time in relation to the phenotype history.

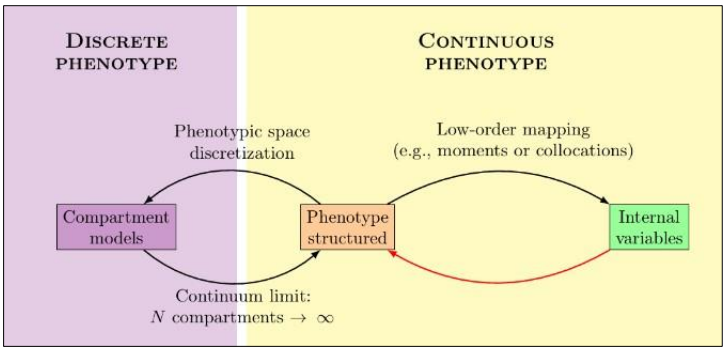

Fig 4: Summary of the different phenotypic plasticity models and how to derive equivalences between them. Red arrows indicate that the transition cannot be accomplished due to lack of information.

while in the Eulerian case it is easier:

1. To monitor the situation at a specific point or phenotype (e.g., how many cells of a given phenotype are present at a given moment, what is the flow of cells of a given phenotype at a specific spatial point).
2. To evaluate flow changes in a steady-state regime.
3. To set "wall" boundaries for movement and phenotype.
4. To solve problems where there are significant changes in position or phenotype, since the initial mesh corresponding to the phenotype domain may become highly distorted.
5. To study abrupt changes in the spatial or temporal evolution of the phenotype (phenotype waves).

The connection between these two formalisms is easy when knowing the movement $\boldsymbol{x}(\boldsymbol{X},t)$ and $\boldsymbol{\xi} = \boldsymbol{\xi}(\boldsymbol{\Xi},t)$ and their inverses $\boldsymbol{X} = \boldsymbol{X}(\boldsymbol{x},t)$ and $\boldsymbol{\Xi} = \boldsymbol{\Xi}(\boldsymbol{\xi},t)$, which is not always possible to obtain in Eulerian formulations.

5. Conclusions

This review integrates biological and mathematical perspectives to elucidate how epigenetic transitions can be modeled across scales. We have traced how successive modeling paradigms, from agent-based to continuum, seek to capture essential features of memory and adaptation. The analogy between physical and biological continua provides not only mathematical tools but also conceptual unity: the same notions of state variables, internal degrees of freedom, and transport apply to materials and to cells.

Among the existing approaches for modeling phenotype as a continuum, which has been proven more biologically consistent, there are two main families. The extra-dimension formulation is powerful for exploring distributional structure, selection, and mixing. It embodies the field perspective, suitable for theoretical analysis of heterogeneity and for deriving macroscopic laws from microscopic mechanisms. The internal-variable formulation captures the same physics in a compressed, interpretable form suitable for practical simulation and integration with other models. Recognizing their equivalence and differences enables modelers to choose the appropriate level of description consciously rather than by convention.

Bridging the two — through theoretical analysis, hybrid modeling, and experimental calibration — will open the way toward a comprehensive, multiscale theory of epigenetic dynamics capable of linking molecular mechanisms to population-level adaptation, and permit to better understand the actual differences between the models found in scientific literature.

Besides, our comparison highlights that the choice between Eulerian and Lagrangian frameworks is a matter of purpose rather than correctness. While the Eulerian description remains the standard for field evolution, a Lagrangian formulation becomes indispensable when tracking individual cellular histories and long-term memory effects.

Future research should also focus on developing hybrid models that combine the strengths of both approaches. Extending internal-variable models to vectorial or tensorial internal spaces, incorporating stochasticity, and coupling them to gene-regulatory dynamics are important avenues for future work. Advances in single-cell multiomics, which can provide snapshots of the epigenetic distribution, will make it possible to estimate model parameters and validate predictions quantitatively. Future extensions may include coupling to stochastic hybrid models, and with dimensionality-reduction techniques to infer the effective epigenetic coordinate from data, and data-driven identification of drift and diffusion terms using physics-informed machine learning [107]. These developments will further strengthen the connection between mathematical modeling and experimental epigenetics, bringing predictive understanding of cellular adaptation closer to clinical application.

Acknowledgments

The authors would like to acknowledge the financial support from Beonchip S.L. through the project DIAMOOC IDI-20220819, the Spanish Research Agency (AEI), through the project PID2021-126051OB-C41 (GBM IMMUNE), the FORT23/00028 project of the ISCIII FORTALECE program, and the Government of Aragon, Spain (group DGA-T62_23R). Manuel Doblare is also grateful for support from the National Foreign Experts Program of China (Grant No. S20250250)

Declaration of Interest Statement

The authors declare that they have no known competing financial interests or personal relationships that could have influenced the work reported in this paper.

CRediT Authorship Contribution Statement

Manuel Doblare: Writing — original draft, Writing — review and editing, Conceptualization, Methodology, Investigation, Formal Analysis, Project administration, Funding acquisition. **Marina Perez-Aliacar:** Writing — review and editing, Methodology, Investigation, Formal Analysis. **Jacobo Ayensa-Jiménez**: Writing — review and editing, Methodology, Investigation, Formal Analysis, Funding acquisition.

Declaration of AI-Based Tool Use

During the preparation of this work Manuel Doblare used Google Gemini in order to help to translate an initial Spanish version to English. After using this tool, Manuel Doblare reviewed and edited the content as needed and takes full responsibility for the content of the publication. Besides, Jacobo Ayensa-Jiménez used Claude Sonnet 4.6 for reviewing the whole paper and the mathematical expressions and to homogenize the notation.

References

1. Alberts B, Johnson A, Lewis J, Morgan D, Raff M, Roberts K, *et al*. Molecular biology of the cell. 6th ed. New York: Garland Science; 2015.
2. Bhat GR, Sethi I, Sadida HQ, Rah B, Mir R, Algehainy N, Albalawi IA, Masoodi T, Subbaraj GK, Jamal F, *et al*. Cancer cell plasticity: from cellular, molecular, and genetic mechanisms to tumor heterogeneity and drug resistance. Cancer Metastasis Rev. 2024;43(1):197-228.
3. Bird A. Perceptions of epigenetics. Nature. 2007; 447:396-8.
4. Allis CD, Jenuwein T. The molecular hallmarks of epigenetic control. Nat Rev Genet. 2016;17(8):487-500.
5. Bale TL. Lifetime stress experience: transgenerational epigenetics and germ cell programming. Dialogues Clin Neurosci. 2014;16(3):297-305.
6. Henikoff S, Greally JM. Epigenetics, cellular memory and gene regulation. Curr Biol. 2016;26(14):R644-8.
7. Atlasi Y, Stunnenberg HG. The interplay of epigenetic marks during stem cell differentiation and development. Nat Rev Genet. 2017;18:643-58.
8. Netea MG, *et al*. Defining trained immunity and its role in health and disease. Nat Rev Immunol. 2020;20:375-88.
9. Flavahan WA, Gaskell E, Bernstein BE. Epigenetic plasticity and the hallmarks of cancer. Science. 2017;357(6348):eaal2380.

10. Feinberg AP. The key role of epigenetics in human disease prevention and mitigation. N Engl J Med. 2018;378:1323-34.
11. Dodd IB, Micheelsen MA, Sneppen K, Thon G. Theoretical analysis of epigenetic cell memory by nucleosome modification. Cell. 2007;129:813-22.
12. Sneppen K, Ringrose L. Theoretical analysis of polycomb-trithorax systems predicts that poised chromatin is bistable and not bivalent. Nat Commun. 2019;10(1):2133.
13. Pérez-Aliacar M, Ayensa-Jiménez J, Doblaré M. Modelling cell adaptation using internal variables: accounting for cell plasticity in continuum mathematical biology. Comput Biol Med. 2023;164:107291.
14. Pérez-Aliacar M, Ayensa-Jiménez J, Ranđelović T, Ochoa I, Doblaré M. Modelling glioblastoma resistance to temozolomide. A mathematical model to simulate cellular adaptation *in vitro*. Comput Biol Med. 2024;180:108866.
15. Celora GL, Byrne HM, Kevrekidis PG. Spatio-temporal modelling of phenotypic heterogeneity in tumour tissues and its impact on radiotherapy treatment. J Theor Biol. 2023;556:111248.
16. Ardaševa A, Gatenby RA, Anderson ARA, Byrne HM, Maini PK, Lorenzi T. A mathematical dissection of the adaptation of cell populations to fluctuating oxygen levels. Bull Math Biol. 2020;82(6):81.
17. Drasdo D, Höhme S. Individual-based approaches to birth and death in avascular tumors. Math Comput Model. 2003;37:1163-75.
18. Rejniak KA, Anderson ARA. Hybrid models of tumor growth. Wiley Interdiscip Rev Syst Biol Med. 2011;3:115-25.
19. Byrne HM, Drasdo D. Individual-based and continuum models of growing cell populations: a comparison. J Math Biol. 2009;58:657-87.
20. Cristini V, Lowengrub J. Multiscale modeling of cancer: an integrated experimental and mathematical approach. Cambridge: Cambridge University Press; 2010.
21. Huang S. The molecular and mathematical basis of Waddington's epigenetic landscape: a framework for post-Darwinian biology? Bioessays. 2012;34:149-57.
22. Furusawa C, Kaneko K. Formation of dominant mode by evolution in biological systems. Phys Rev E. 2018;97(4):042410.
23. França GS, Baron M, King BR, Bossowski JP, Bjornberg A, Pour M, *et al*. Cellular adaptation to cancer therapy along a resistance continuum. Nature. 2024;631(8022):876-83.
24. Mandal M, Ghosh B, Anura A, Mitra P, Pathak T, Chatterjee J. Modeling continuum of epithelial mesenchymal transition plasticity. Integr Biol. 2016;8(2):167-76.
25. Celora GL, Byrne HM, Zois CE, Kevrekidis PG. Phenotypic variation modulates the growth dynamics and response to radiotherapy of solid tumours under normoxia and hypoxia. J Theor Biol. 2021;527:110792.
26. Anderson ARA, Chaplain MAJ. Continuous and discrete mathematical models of tumor-induced angiogenesis. Bull Math Biol. 1998;60:857-99.
27. Murray JD. Mathematical biology: I. An introduction. 3rd ed. New York: Springer; 2002.
28. Byrne HM. Dissecting cancer through mathematics: from the cell to the animal model. Nat Rev Cancer. 2010;10:221-30.
29. Fletcher AG, Osterfield M, Baker RE, Shvartsman SY. Vertex models of epithelial morphogenesis. Biophys J. 2014;106:2291-304.
30. Caicedo JC, *et al*. Evaluation of deep learning strategies for nucleus segmentation in fluorescence images. Cytometry A. 2019;95:952-65.
31. Saad M, He S, Thorstad W, Gay H, Barnett D, Zhao Y, *et al*. Learning-based cancer treatment outcome prognosis using multimodal biomarkers. IEEE Trans Radiat Plasma Med Sci. 2021;6(2):231-44.
32. Rodrigues JA. Using physics-informed neural networks (PINNs) for tumor cell growth modeling. Mathematics. 2024;12(8):1195.
33. El Afari W, Ziani M, Assaoui F. Tumor propagation modeling using physics-informed neural networks and variational methods for MRI image segmentation. J Math Imaging Vis. 2026;68(2):8.
34. Railsback S, Grimm V. Agent-based and individual-based modeling: a practical introduction. Princeton: Princeton University Press; 2011.
35. Colyer B, Bak M, Basanta D, Noble R. A seven-step guide to spatial, agent-based modelling of tumour evolution. Evol Appl. 2024;17(5):e13687.
36. Wang Z, Butner JD, Kerketta R, Cristini V, Deisboeck TS. Simulating cancer growth with multiscale agent-based modeling. Semin Cancer Biol. 2015;30:70-8.
37. Bull JA, Byrne HM. Quantification of spatial and phenotypic heterogeneity in an agent-based model of tumour-macrophage interactions. PLoS Comput Biol. 2023;19(3):e1010994.
38. Deutsch A, Dormann S. Cellular automaton modeling of biological pattern formation: characterization, applications, and analysis. 2nd ed. Basel: Birkhäuser; 2017.
39. Osborne JM, Fletcher AG, Pitt-Francis JM, Maini PK, Gavaghan DJ. Comparing individual-based approaches to modelling the self-organization of multicellular tissues. PLoS Comput Biol. 2017;13(2):e1005387.
40. Truesdell C, Noll W. The non-linear field theories of mechanics. 3rd ed. Berlin: Springer; 2004.
41. Gurtin ME, Fried E, Anand L. The mechanics and thermodynamics of continua. Cambridge: Cambridge University Press; 2010.
42. Ayensa-Jiménez J, Pérez-Aliacar M, Randelovic T, *et al*. Mathematical formulation and parametric analysis of *in vitro* cell models in microfluidic devices: application to different stages of glioblastoma evolution. Sci Rep. 2020;10(1):21193.
43. Turing AM. The chemical basis of morphogenesis. Philos Trans R Soc Lond B Biol Sci. 1952;237:37-72.
44. Swanson KR, Rockne RC, Claridge J, Chaplain MA, Alvord EC Jr, Anderson ARA. Quantifying the role of angiogenesis in malignant progression of gliomas: in silico modeling integrates imaging and histology. Cancer Res. 2011;71(24):7366-75.
45. Chaplain MAJ, Lolas G. Mathematical modelling of cancer invasion of tissue: dynamic heterogeneity. Netw Heterog Media. 2006;1(3):399-439.
46. Malvern LE. Introduction to the mechanics of a continuous medium. Englewood Cliffs: Prentice-Hall; 1969.
47. Bird RB, Stewart WE, Lightfoot EN. Transport phenomena. 2nd ed. New York: Wiley; 2001.
48. Duncan EJ, Gluckman PD, Dearden PK. Epigenetics, plasticity, and evolution: how do we link epigenetic change to phenotype? J Exp Zool B Mol Dev Evol. 2014;322(4):208-20.
49. Jaenisch R, Bird A. Epigenetic regulation of gene expression: how the genome integrates intrinsic and environmental signals. Nat Genet. 2003;33(3 Suppl):245-54.
50. Kim JK, Samaranayake M, Pradhan S. Epigenetic mechanisms in mammals. Cell Mol Life Sci. 2009;66:596-612.

51. Sharma S, Kelly TK, Jones PA. Epigenetics in cancer. Carcinogenesis. 2010;31(1):27-36.
52. Ferrell JE. Self-perpetuating states in signal transduction: positive feedback, double-negative feedback and bistability. Curr Opin Cell Biol. 2002;14:140-8.
53. Kaern M, Elston TC, Blake WJ, Collins JJ. Stochasticity in gene expression: from theories to phenotypes. Nat Rev Genet. 2005;6:451-64.
54. Gupta PB, *et al*. Stochastic state transitions give rise to phenotypic equilibrium in populations of cancer cells. Cell. 2011;146:633-44.
55. Pisco AO, *et al*. Non-Darwinian dynamics in therapy-induced cancer drug resistance. Nat Commun. 2013;4:2467.
56. Bintu L, Yong J, Antebi YE, McCue K, Kazuki Y, Uno N, *et al*. Dynamics of epigenetic regulation at the single-cell level. Science. 2016;351(6274):720-4.
57. Bukkuri A, Brown JS. Integrating eco-evolutionary dynamics into matrix population models for structured populations: discrete and continuous frameworks. Methods Ecol Evol. 2023;14(6):1475-88.
58. Caswell H, de Vries C, Hartemink N, Roth G, van Daalen SF. Age × stage-classified demographic analysis: a comprehensive approach. Ecol Monogr. 2018;88(4):560-84.
59. Jongejans E, Huber H, de Kroon H. Scaling up phenotypic plasticity with hierarchical population models. Evol Ecol. 2010;24(3):585-99.
60. Jiménez-Sánchez J, Martínez-Rubio Á, Popov A, Pérez-Beteta J, Azimzade Y, Molina-García D, *et al*. A mesoscopic simulator to uncover heterogeneity and evolutionary dynamics in tumors. PLoS Comput Biol. 2021;17(2):e1008266.
61. Strobl MAR, West J, Viossat Y, Damaghi M, Robertson-Tessi M, Brown JS, *et al*. Turnover modulates the need for a cost of resistance in adaptive therapy. Cancer Res. 2021;81(4):1135-47.
62. McDermott M, Mehta R, Roussos Torres ET, MacLean AL. Modeling the dynamics of EMT reveals genes associated with pan-cancer intermediate states and plasticity. NPJ Syst Biol Appl. 2025;11(1):31.
63. Lacroix D, Prendergast P. A mechano-regulation model for tissue differentiation during fracture healing: analysis of gap size and loading. J Biomech. 2002;35(9):1163-71.
64. Pivonka P, Zimak J, Smith DW, Gardiner BS, Dunstan CR, Sims NA, *et al*. Model structure and control of bone remodeling: a theoretical study. Bone. 2008;43(2):249-63.
65. Lemaire V, Tobin FL, Greller LD, Cho CR, Suva LJ. Modeling the interactions between osteoblast and osteoclast activities in bone remodeling. J Theor Biol. 2004;229(3):293-309.
66. Rocha HL, Godet I, Kurtoglu F, Metzcar J, Konstantinopoulos K, Bhoyar S, *et al*. A persistent invasive phenotype in post-hypoxic tumor cells is revealed by fate mapping and computational modeling. iScience. 2021;24(9).
67. Ayuso JM, Monge R, Martínez-González A, Virumbrales-Muñoz M, Llamazares GA, Berganzo J, *et al*. Glioblastoma on a microfluidic chip: generating pseudopalisades and enhancing aggressiveness through blood vessel obstruction events. Neuro Oncol. 2017;19(4):503-13.
68. Johnson KE, Howard GR, Morgan D, Brenner EA, Gardner AL, Durrett RE, *et al*. Integrating transcriptomics and bulk time course data into a mathematical framework to describe and predict therapeutic resistance in cancer. Phys Biol. 2020;18(1):016001.
69. Ollier E, Mazzocco P, Ricard D, Kaloshi G, Idbaih A, Alentorn A, *et al*. Analysis of temozolomide resistance in low-grade gliomas using a mechanistic mathematical model. Fundam Clin Pharmacol. 2017;31(3):347-58.
70. Greene JM, Gevertz JL, Sontag ED. Mathematical approach to differentiate spontaneous and induced evolution to drug resistance during cancer treatment. JCO Clin Cancer Inform. 2019;3:1-20.
71. Russo M, Pompei S, Sogari A, Corigliano M, Crisafulli G, Puliafito A, *et al*. A modified fluctuation-test framework characterizes the population dynamics and mutation rate of colorectal cancer persister cells. Nat Genet. 2022;54(7):976-84.
72. Gunnarsson EB, De S, Leder K, Foo J. Understanding the role of phenotypic switching in cancer drug resistance. J Theor Biol. 2020;490:110162.
73. Hamis S, Browning AP, Jenner AL, Villa C, Maini PK, Cassidy T. Growth rate-driven modelling suggests that phenotypic adaptation drives drug resistance in BRAFV600E-mutant melanoma. Commun Biol. 2026;9:385. doi:10.1038/s42003-026-09760-2.
74. Staňková K, Brown JS, Dalton WS, Gatenby RA. Optimizing cancer treatment using game theory: a review. JAMA Oncol. 2019;5(1).
75. Basanta D, Scott JG, Fishman MN, Ayala G, Hayward SW, Anderson ARA. Investigating prostate cancer tumour–stroma interactions: clinical and biological insights from an evolutionary game. Br J Cancer. 2012;106(1):174-81.
76. Lorenzi T, Chisholm RH, Clairambault J. Tracking the evolution of cancer cell populations through the mathematical lens of phenotype-structured equations. Biol Direct. 2016;11(1):43.
77. Chisholm RH, Lorenzi T, Desvillettes L, Hughes BD. Evolutionary dynamics of phenotype-structured populations: from individual-level mechanisms to population-level consequences. Z Angew Math Phys. 2016;67(4):100.
78. Chiari G, Fiandaca G, Delitala ME. Hypoxia-resistance heterogeneity in tumours: the impact of geometrical characterization of environmental niches and evolutionary trade-offs. A mathematical approach. Math Model Nat Phenom. 2023;18:18.
79. Fiandaca G, Bernardi S, Scianna M, Delitala ME. A phenotype-structured model to reproduce the avascular growth of a tumor and its interaction with the surrounding environment. J Theor Biol. 2022;535:110980.
80. Greene J, Lavi O, Gottesman MM, Levy D. The impact of cell density and mutations in a model of multidrug resistance in solid tumors. Bull Math Biol. 2014;76(3):627-53.
81. Lorenzi T, Chisholm RH, Desvillettes L, Hughes BD. Dissecting the dynamics of epigenetic changes in phenotype-structured populations exposed to fluctuating environments. J Theor Biol. 2015;386:166-76.
82. Stace REA, Stiehl T, Chaplain MAJ, Marciniak-Czochra A, Lorenzi T. Discrete and continuum phenotype-structured models for the evolution of cancer cell populations under chemotherapy. Math Model Nat Phenom. 2020;15:14.
83. Lorenzi T, Painter KJ, Villa C. Phenotype structuring in collective cell migration: a tutorial of mathematical models and methods. J Math Biol. 2025;90(6):61.
84. Brogan WL. Modern control theory. Pearson Education India; 1991.
85. Horstemeyer MF, Bammann DJ. Historical review of internal state variable theory for inelasticity. Int J Plast. 2010;26(9):1310-34.
86. Coleman BD, Gurtin ME. Thermodynamics with internal state variables. J Chem Phys. 1967;47(2):597-613.

87. Maugin GA. The thermomechanics of nonlinear irreversible behaviors: an introduction. Singapore: World Scientific; 1999
88. Yu JS, Bagheri N. Agent-based models predict emergent behavior of heterogeneous cell populations in dynamic microenvironments. Front Bioeng Biotechnol. 2020;8:249.
89. Kieu M, Malleson N, Heppenstall A. Dealing with uncertainty in agent-based models for short-term predictions. R Soc Open Sci. 2020;7:191074.
90. Robin TT, Cascante-Vega J, Shaman J, Pei S. System identifiability in a time-evolving agent-based model. PLoS One. 2024;19(1):e0290821.
91. McCulloch J, Ge J, Ward JA, Heppenstall A, Polhill JG, Malleson N. Calibrating agent-based models using uncertainty quantification methods. J Artif Soc Soc Simul. 2022;25(2).
92. Bonabeau E. Agent-based modeling: methods and techniques for simulating human systems. Proc Natl Acad Sci U S A. 2002;99(Suppl 3):7280-7.
93. Lorz A, Lorenzi T, Hochberg ME, Clairambault J, Perthame B. Populational adaptive evolution, chemotherapeutic resistance and multiple anti-cancer therapies. ESAIM Math Model Numer Anal. 2013;47(2):377-99.
94. Cilfone NA, Kirschner DE, Linderman JJ. Strategies for efficient numerical implementation of hybrid multi-scale agent-based models to describe biological systems. Cell Mol Bioeng. 2015;8(1):119-36.
95. Nardini JT, Baker RE, Simpson MJ, Flores KB. Learning differential equation models from stochastic agent-based model simulations. J R Soc Interface. 2021;18(176).
96. Anderson ARA. A hybrid discrete-continuum technique for individual-based migration models. In: Polymer and cell dynamics: multiscale modeling and numerical simulations. Berlin: Springer; 2003. p. 251-9.
97. de la Cruz R, Guerrero P, Calvo J, Alarcón T. Coarse-graining and hybrid methods for efficient simulation of stochastic multi-scale models of tumour growth. J Comput Phys. 2017;350:974-91.
98. Stevens A. The derivation of chemotaxis equations as limit dynamics of moderately interacting stochastic many-particle systems. SIAM J Appl Math. 2000;61(1):183-212.
99. Drasdo D. Coarse graining in simulated cell populations. Adv Complex Syst. 2005;8(2-3):319-63.
100. Murray PJ, Edwards CM, Tindall MJ, Maini PK. From a discrete to a continuum model of cell dynamics in one dimension. Phys Rev E Stat Nonlin Soft Matter Phys. 2009;80(3):031912.
101. Hillen T, Painter KJ. A user's guide to PDE models for chemotaxis. J Math Biol. 2009;58(1):183-217.
102. Van Liedekerke P, Palm MM, Jagiella N, Drasdo D. Simulating tissue mechanics with agent-based models: concepts, perspectives and some novel results. Comput Part Mech. 2015;2(4):401-44.
103. Arroyo-Vázquez RB, Pérez-Aliacar M, Ayensa-Jiménez J, Doblaré M. On the equivalence between agent-based and continuum models for cell population modeling. Application to glioblastoma evolution in microfluidic devices. bioRxiv. 2024. doi: 10.1101/2024.09.05.611243.
104. Ayuso JM, Virumbrales-Muñoz M, Lacueva A, Lanuza PM, Checa-Chavarria E, Botella P, *et al*. Development and characterization of a microfluidic model of the tumour microenvironment. Sci Rep. 2016;6:36086.
105. Ardaševa A, Anderson ARA, Gatenby RA, Byrne HM, Maini PK, Lorenzi T. Comparative study between discrete and continuum models for the evolution of competing phenotype-structured cell populations in dynamical environments. Phys Rev E. 2020;102(4):042404.
106. Buenrostro JD, Corces MR, Lareau CA, Wu B, Schep AN, *et al*. Integrated single-cell analysis maps the continuous regulatory landscape of human hematopoiesis. Cell. 2018;173:1535-48.
107. Ayensa-Jiménez J, Doweidar MH, Sanz-Herrera JA, Doblare M. Understanding glioblastoma invasion using physically-guided neural networks with internal variables. PLoS Comput Biol. 2022;18(4):e1010019.

How to Cite This Article

Doblaré M, Pérez-Aliacar M, Ayensa-Jiménez J. Modeling cell dynamics and epigenetic transitions: From agent-based to transport frameworks. Journal of Frontiers in Multidisciplinary Research. 2026;7(2):242-258. doi:10.54660/.JFMR.2026.7.2.242-258.

Creative Commons (CC) License

This is an open access journal, and articles are distributed under the terms of the Creative Commons Attribution NonCommercial-ShareAlike 4.0 International (CC BY-NC-SA 4.0) License, which allows others to remix, tweak, and build upon the work non-commercially, as long as appropriate credit is given and the new creations are licensed under the identical terms